AN INVESTIGATION INTO THE EFFECTS OF VARIATION OF PARTICLE SIZE ON THE FLUIDIZATION AND DE-AERATION CHARACTERISTICS OF POWDERS TO ASSESS DENSE-PHASE PNEUMATIC CONVEYABILITY

A
Thesis

submitted in partial fulfillment of the requirements for the award of degree of

Master of Engineering (M.E.)

In
Thermal Engineering

Submitted by
AMANPREET CHAWLA
(ROLL NO. 801383001)

UNDER THE GUIDANCE OF

Dr. S.S. MALLICK

(Assistant Professor)

DEPARTMENT OF MECHANICAL ENGINEERING
THAPAR UNIVERSITY, PATIALA – 147004
JULY 2015

CERTIFICATION

I, Amanpreet Chawla, declare that this thesis report entitled "***An Investigation into the Effects of Variation of Particle Size on Fluidization and De-aeration Characteristics of Powders to Assess Dense-Phase Pneumatic Conveyability***", submitted towards fulfillment of the requirements for the award of Master's Degree in Thermal Engineering, in Mechanical Engineering Department of Thapar University, Patiala, is entirely my own work. This document has not been submitted for any degree in any other institution.

Amanpreet Chawla

Date: 14/07/2015

Place: Patiala

Amanpreet Chawla

801383001

Thapar University, Patiala

This is to certify that above statement made by the candidate is correct and true to the best of my knowledge.

Dr. S.S. Mallick

(Assistant Professor)

Mechanical Engineering Department

Thapar University, Patiala

Countersigned by

Dr. S.K. Mohapatra

Sr. Professor and Head

Mechanical Engineering Department

Thapar University, Patiala

Dr. S.S. Bhatia

Dean

Academic Affairs

Thapar University, Patiala

ACKNOWLEDGEMENT

I would like to express my special appreciation to my supervisor, Dr. S.S. Mallick, for teaching me how to be a researcher, guiding me with patience, and encouraging me all the time. His enthusiasm, encouragement and faith in me throughout have been extremely helpful. He was always available for my questions, was positive and gave his time generously. I would like to acknowledge all the members of mechanical workshops, Thapar University, for their help and suggestions in fabrication of test equipment. A special thanks of note to Mr. Gautam Setia, Research Scholar for their expert guidance.

A special debt of gratitude is owed to the authors whose work I have consulted and quoted in this work. Last but not the least, I am forever grateful to my parents, family and friends for their unconditional support and best wishes.

ABSTRACT

This thesis results from an ongoing investigation carried out into the effects of differences in particle size distribution on the fluidization and de-aeration characteristics of seven different samples of fly ash (d_{50}: 21-139 µm) collected from different ESP hoppers of same unit of a coal fired thermal power station. An experimental facility was developed for testing the fluidization and deaeration characteristics. It was found that the minimum fluidization velocity decreased quite considerably with the reduction in median particle size from 139 to 102 µm. Further reduction in particle size to 21 µm resulted in an increment in minimum fluidization velocity because of the stronger inter-particle cohesive forces that are prevalent in smaller sized particles. De-aeration test results showed that the sample with largest particle size (139 µm) has the least ability to retain air due to higher permeability. The smallest particle sized particles (21µm) showed a gradual decrease in relative bed height and pressure drop per unit length with time indicating higher air retention capacities. It was found that the experimental value of minimum fluidization velocity for the finer 21µm sized fly ash (Geldart Group C powder) was larger than that predicted by the popular existing models. It is concluded that the 139 µm sized fly ash is a dilute-phase product, whereas fly ash samples with particle size varying from 69 to 21 µm have dense-phase conveyability due to higher air retention capacities.

TABLE OF CONTENTS

List of Figures

List of tables

List of Symbols

A_f	Mainwaring de-aeration factor [Pa s m^{-1}]
Ar	Archimedes number
d_P	Particle diameter [µm]
d_{50}	Particle median diameter [µm]
E_G	Gravitational-force factor
E_C	Cohesive force factor
Fr	Froude number
Grt	Sanchez et. al de-aeration factor
g	Acceleration due to gravity [ms^{-2}]
K'v	Jones de-aeration rate constant [ms^{-1}]
Lo	Initial bed height [m]
L	Bed height [m]
P*	Sanchez et.al permeability factor
ΔP	Pressure drop [kPa]
Re	Reynolds number
Re_{mf}	Reynolds number at minimum fluidization velocity
T	Time [s]
U	Gas velocity [ms^{-1}]
U_{mf}	Minimum fluidization velocity [ms^{-1}]
U_{mb}	Minimum bubbling velocity [ms^{-1}]

ε_{mf} Voidage at minimum fluidization velocity

ρ_{bl} Loose poured bulk density [kgm^{-3}]

ρ_g Fluid density [kgm^{-3}]

ρ_s Particle density [kgm^{-3}]

μ_g Fluid viscosity [Pa.s]

φ_s Sphericity

Ψ Permeability factor [m^3 s kg^{-1}]

λ Internal friction factor

Abbreviations

ESP Electro Static Precipitator

FCC Fluidized Cracking Catalyst

PSD Particle Size distribution

SEM Scanning Electron Microscope

VFD Variable Frequency Drive

CHAPTER 1: INTRODUCTION AND OBJECTIVES

1.1 Introduction

Pneumatic conveying is the process of transportation of bulk materials such as cement, fly ash etc. by using compressed air/ gas or vacuum as conveying medium through an enclosed flow channel from one place to another (Wypych, 2006). The major advantages of pneumatic conveying are flexibility, confined flow, dust free, ability to distribute materials from one source to another and also pick up materials from different locations, automation, low maintenance cost etc. In the past, only dilute phase mode of transport was used for conveying, in which particles remain suspended with the fluid stream and it is also known as suspended flow.This mode of conveying leads to high power consumption and high maintenance cost of the system. To overcome these problems, dense phase pneumatic conveying system are nowadays employed (Klinzing et al., 2009). Fluidized dense phase pneumatic conveying of powders is gaining popularity in industries, e.g. thermal power plants, cement, pharmaceuticals, advanced material, chemical etc, due to its various advantages such as reduced air flow, reduced gas velocity, higher solids to air mass ratio, reduced size requirement of gas- solid separator unit etc (Mallick, 2009) . Fine powders, typically Geldart type A powders, such as fly ash, cement, pulverized coal, FCC etc, which have good fluidizing and air- retention characteristics are conveyed in fluidized dense phase flow. The designing of fluidized dense phase pneumatic conveying system is based on the estimation of two main parameters - total pipeline pressure drop and minimum air flow rate requirement. Accurate prediction of these two design parameters is necessary for the reliable operation of pneumatic conveying systems. Under-prediction of total pipeline pressure drop would lead to reduced material flow rate and under-estimation of reliable transport boundary could cause saltation in pipe, product builds up, unstable flow and eventually pipeline blockage (Wypych, 1989). In case of over-prediction of these two parameters, this could lead to higher air velocity requirement, high wear rate of pipelines and attrition of materials .

Researchers and designers have achieved considerable amount of success in modeling dilute-phase flow, where the principles of suspension flow can be applied rather easily. Relatively, modeling of the flow behavior of fluidized dense phase pneumatic conveying system remains a noteworthy challenge to the researchers, as fluidized dense phase pneumatic conveying system consists of highly turbulent concentrated bed of powders moving through horizontal pipe. Due to the complex nature of the flow, basic modeling of key design parameters (Mallick, 2009) e.g solid friction factor and minimum transport boundary, have remained to be a significant task. Therefore over the years, researchers have used power function type models to represent these parameters. These models have used several dimensionless parameters such as m^*, Fr, $\frac{\rho_g}{\rho_s}$, $\frac{d_{50}}{D}$ etc. These models have shown good fit in researchers' own data. However, these models have shown inaccuracy when tested under proper scale up condition (Wypych, 1989). This is because the existing models do not fundamentally address the flow mechanism of the powders being conveyed in fluidized dense phase flow.

Fluidization and de-aeration characteristics are considered to be important fundamental parameters to understand the flow behavior of powders. Mainwaring and Reed (1987) worked on 13 different materials ranging from coarse pellets to fine pulverized coal to relate the two above characteristics with the flow modes of dense phase pneumatic conveying and found that two different flow mechanisms – plug flow and moving bed flow are prevalent. High permeability materials tend to flow in plug mode, whereas material with good air retention capability tends to flow in moving bed condition. Xie and Geldart (1995) carried out experiments on FCC powders of different particle size ranging from 26 to 137 μm to study the fluidization behavior by taking into effect of the type of gas and temperature. They also compared the minimum fluidization velocity with three well known correlation reported in literature and anticipated the new

improved correlation for U_{mb} based upon regression analysis of experimental data for temperature up to 500 ^{o}C and with ± 20% accuracy. Jones and Williams (2008) developed a new two dimensional diagram that could predict the three pneumatic conveying flow modes without the need to determine the de-aeration values. The diagram was plotted between loose poured density and permeability because of the difficulties experienced in determining de-aeration factor. Xu and Zhu (2008) worked on the fluidization characteristics of FCC and glass beads of different sizes and anticipated new correlation to find out the minimum fluidization velocity (U_{mf}) considering the degree of cohesiveness of materials by taking into effect the relative inter-particle forces between particles. Liu et al. (2015) studied the fluidization behavior of superfine particles with mean diameter of 5.181 μm of silica (SiO_2). The minimum fluidization velocity was found based on the agglomerate formation of particles which was studied with the help of 2D Particle Image Velocimeter. They also worked on the bed collapse experiment to determine the fluidization regimes. It can be imagined that powders that have higher capacity of retaining air would be transported with more ease than a powder that would de-aerate faster. Therefore, a fundamental approach would involve an evaluation of fluidizing and de-aeration characteristics of powders and to determine its relation to the respective pneumatic conveying characteristics.

1.2 Objectives

Specific objectives include:

i. To study the effect of particle size on the fluidizing characteristics of fine powders.

ii. To study the effect of particle size on the de-aeration characteristics of fine powders.

iii. To evaluate different existing minimum fluidization velocity correlations by comparing with experimental data.

CHAPTER 2: LITERATURE REVIEW

This chapter includes the basic components of pneumatic conveying system, material classification diagrams, material characteristics, fluid- particle characteristics and extensive literature review carried out by different researchers on fluidization and de-aeration characteristics of bulk solid. Also, various empirical and theoretical correlations of minimum fluidization velocity are also presented.

2.1 Basic components of pneumatic conveying systems

Basic components of pneumatic conveying systems are as follows:-

1. *Prime movers:*

   Prime movers are devices which supplies the air/ gas at required pressure. Various types of prime movers are available, such as compressors, blowers and fans to provide the conveying gas. Depending on the requirement of the system, whether to have positive or negative pressure systems, these movers are installed accordingly.

2. *Feeding devices:*

   It is the most critical zone in pneumatic conveying system where the majority of problems occurs due to mismatch of feeder characteristics and prime mover. Various types of feeding devices are rotary valves, venturi, screw feeders, blow tank, vacuum nozzle etc. The selection of feeding devices depends upon the pressure drop in the line and also on materials to be conveyed in the line (Wypych, 2006).

3. *Conveying line:*

   This consists of pipeline in which materials are conveyed from a feeding device to the bin where it is stored. A pipeline consists of a horizontal pipe, vertical pipe, many bends. The selection of piping materials depends upon many factors such as pressure requirement, product properties and abrasiveness of the materials.

4. *Solids-gas separator:*

   Many separators such cyclone separator, bag filters are available, which are used to separate gas/air and the product from the conveying system (Wypych, 2006). These separators are employed at the end of pipelines and top of the bin before entering. The fabric filter is employed for fine powders, cyclone separators are employed for wide particle size distribution and granular materials. For the continuous operation of these devices special type of device known as reverse jet cleaning is employed in the system.

2.2 Material classification diagrams

2.2.1 Geldart fluidization classification diagram

Geldart (1973), according to the fluidization behavior of bulk materials, developed a classification diagram and segregated powders into following four groups depending on particle diameter (d_p) and density difference (Klinzing et al., 2009):

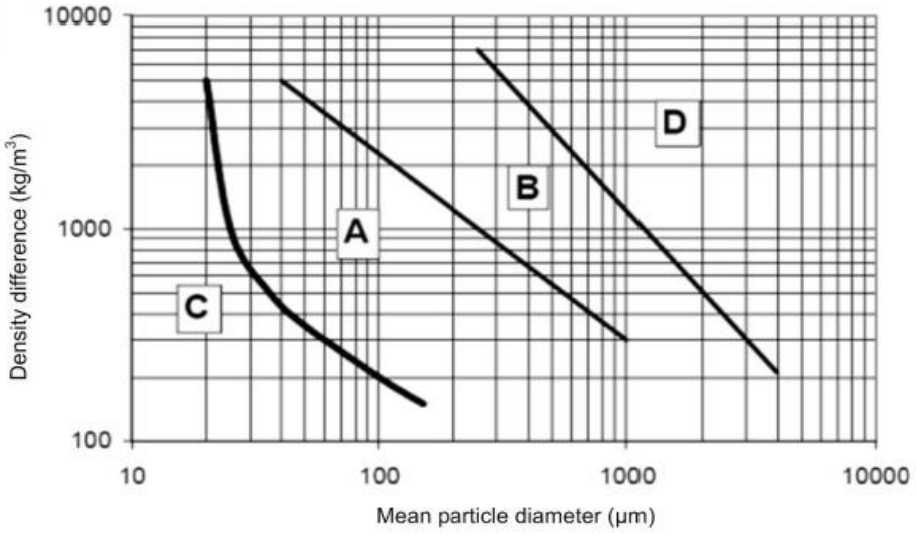

Figure 2.1 Geldart Classification Diagram (Klinzing et al., 2009)

Group A: Powders lying in this group easily get aerated and have ability to retain fluidization characteristics. This group of powders are characterized by the ratio of minimum bubbling velocity (U_{mb}) and minimum fluidization velocity (U_{mf}) and for this group the ratio is defined as (U_{mb}/U_{mf}) >1. The bed collapses very slowly when gas supply is turned off.

Group B: Powders lying in this group fluidize readily and has a tendency to form bubbles when velocity is increased to U_{mf} .This group is characterized by ($U_{mb} = U_{mf}$). The bed collapses very quickly when the gas supply is turned off.

Group C: Powders lying in this group are cohesive in nature and are difficult to be fluidized. In this group fluidized bed is lifted in the form solid plugs separated by fluidizing gas. Powders can be easily fluidized by using external sources such as vibrations, stirring etc.

Group D: Powders lying in this group are large sized particle and having high particle density. Larger gas velocity is required to fluidize the materials as compared to Group B particles. These

are also known as spoutable powders because of ability to form stable spouts when gas is introduced in powders in proper manner.

2.2.2 Dixon slugging diagram

Dixon (1979) discovered that fluidization characteristics of the material were important to know the convey ability of the product in dense phase. Based on the ability of a material to form slugs in dense phase vertical transport system, Dixon (1979) developed a classification diagram for pneumatic conveying system. The diagram was drawn between the same axes as Geldart diagram with boundaries between expected flow conditions. Dixon concluded the four slugging categories and relates well to Geldart boundaries:

Group A powders generally show no slug formation and were good candidate for dense phase pneumatic conveying. They have the ability to achieve high solid/-gas loading.

Group B powders can cause problems such as vibration in pipeline if attempt was made to convey the product at high solid/ gas loading.

Group C powders generally show channeling during fluidization due to cohesive nature of material thus leads to poor fluidization characteristics, but these powders may have good potential for dense phase pneumatic conveying as boundary A-C was imprecise.

Group D powders form strong axisymmetric slug thus it may be suitable for dense phase, but these powders have relatively less solid loading ratio than Group A powders and it can be conveyed at high solid loading than Group B powders.

2.3 Basic particle characteristics:

Particle size distribution

Various methods are available to determine size distribution such as mechanical sieving, laser diffraction and sedimentation. Mechanical sieving method is commonly used to determine the size. The most important parameter determined from this particle size distribution is median size/mean particle size which is calculated from either mass or volumetric analysis and it also depends on the measuring technique (Kennedy and Wypych, 2006).

Particle density

It is a significant parameter in pneumatic conveying because of its effect on pick-up velocity. It is defined as the ratio of known mass of material to known volume of the material. It can be determined by using specific gravity bottle or by using pycnometer.

Bulk density

The Bulk density is the measure of average density of the material. It is possible to obtain a number of densities (tapped density, loose poured density, consolidated density) depending on the amount of compaction or expansion. Bulk density is also a function of particle size distribution (Kennedy and Wypych, 2006).

2.4 Fluid – particle interaction

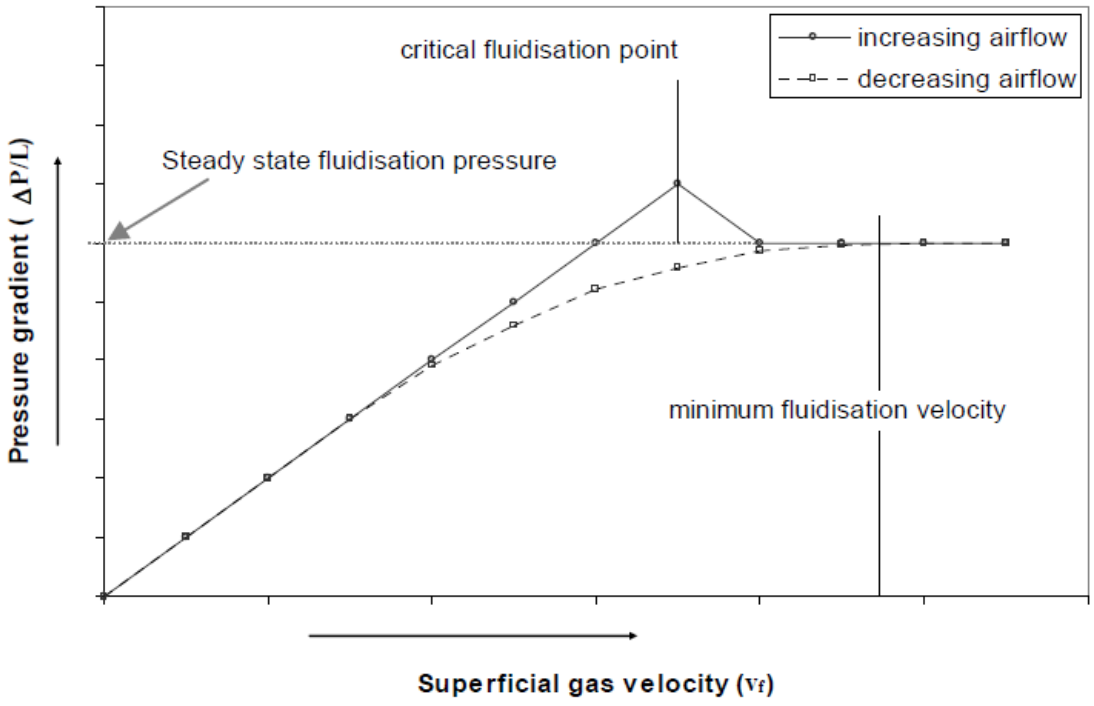

Figure 2.2: Ideal fluidization diagram (Williams, 2008)

Fluidization

It refers to mixing of gas/air with bulk solids so that it behaves like a fluid. The minimum superficial velocity required by gas to make bulk solid act like a fluid is known as minimum fluidization velocity (U_{mf}). Minimum fluidization velocity is determined from the fluidization curve which shows the variation of pressure gradient across the material bed (i.e. pressure drop per unit bed height) against superficial air velocity (Wypych, 2006).

Steady state fluidization pressure

It may be defined as fluidization pressure whose value becomes relatively constant for increasing or decreasing gas velocities.

Permeability

It can be defined as rate at which air can permeate through fixed bed of bulk materials (Sanchez et al, 2003). It is also defined as ability to allow air to fill and flow through the voids which occurs due different size of bulk solids during pouring (Jones and Williams, 2008). The permeability factor (Ψ) is defined as slope of linear part up to U_{mf} of fluidization curve. Permeability of bulk solids can be measured by standard fluidization tests or by using permeameter. It was found that materials having high permeability are capable of plug flow and low permeability materials are capable of moving bed flow.

De-aeration

It can be defined as the ability of gas/air to leave the fluidized bed when air supply is turned off or when fluidized material has been conveyed into the bin (Kennedy and Wypych, 2006). De-aeration may be measured by recording the collapse in the bed height as the air escapes out of material bed or more expediently by recording the pressure drop per unit length against time after shutting off the air supply. The de-aeration behavior of material provides useful information about the ability of material to retain air which depends on various factors, such as particle size or shape, porosity, density etc. The exponential rate of decay in pressure gradient was seen in many materials. Therefore it allows to determine the characteristic time constant for every material (Wypych, 2006).

From pneumatic conveying point of view it could be concluded that the longer it takes a for bulk solid to de-aerate means it retains the fluid like properties and it will easily move in conveying pipeline. This air- retention property helps to solve the problems related to the flow of powders.

2.5 Fluidization test

It consists of a vertical column of specific height made of mainly Perspex tube materials along the periphery of the tube pressure transducers are installed to measure the pressure drop and under this there is a distribution plate and plenum chamber which allow air/gas from prime mover to pass through bulk materials in the column. In this test air/gas allowed to flow upwards through the column filled with bulk materials with the equilibrium pressure measured across the bed. The flow of air/ gas is increased or decreased and pressure drop is recorded simultaneously and then pressure drop vs. superficial velocity is plotted in order to get the fluidization behavior of bulk solids.

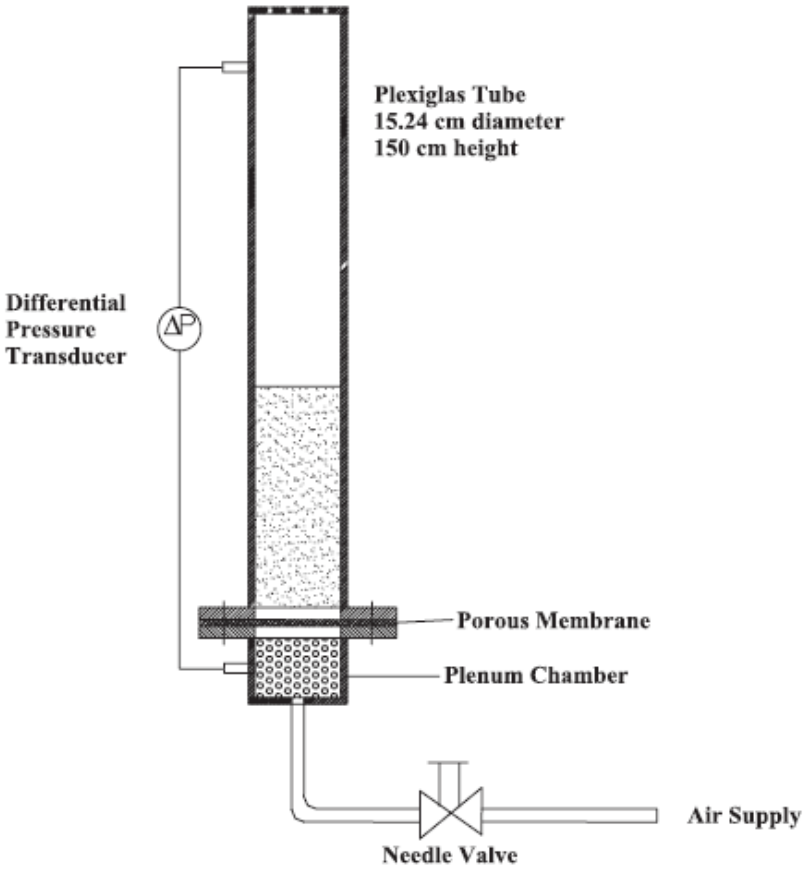

Figure 2.3: Fluidization Standard Test Rig (Sanchez et.al, 2003)

2.6 Review of previous research work

Mainwaring and Reed (1987) developed two diagram prognostic techniques for dense phase pneumatic conveying capability based on two important air/particle factors i.e. Permeability and De-aeration, which comprised of determining the steady state fludisation pressure ($\Delta P/L$) and permeability of the material by using a permeameter. Mainwaring defined the De-aeration factor (A_f) on the basis of the rate of change of pressure drop per unit length against time after shutting off the air. The relationship between pressure drop and time was obtained by using best fit approach.

The first diagram was drawn between permeability factor and steady state fludisation pressure. It was found that low permeability materials show dilute phase and fluidized dense phase whereas, high permeability materials shows plug flow. He defined constant U_{mf} line of 50 mm/s and proposed that materials above this line are capable of plug flow. The second diagram was drawn between De-aeration constant divide by the particle density and steady state fluidization pressure. They proposed that bulk materials which have high air retention are good candidates for fluidized dense phase if their points lies above X=0.001 m^3s/kg.

Jones and Mills (1990) developed a model for product classification in pneumatic conveying based on permeability and de-aeration. The main difference between Jones (1990) models from Mainwaring (1987) model is that only one diagram was used to determine various mode of flows. Jones (1990) used the same procedure to determine the permeability of different materials but for the de-aeration value they used vibrated de-aeration constant (K'v) instead of Mainwaring's constant of de-aeration. The vibrated de-aeration value related to rate of change in

bed height of a column of bulk material to the consolidated vibrated state defined by equation 2.1:

$$\frac{d\rho_b}{dt} = K'v \frac{\Delta\rho_b}{L} \qquad (2.1)$$

Jones (1990) model diagram was drawn between de-aeration rate constant (K'v) and permeability factor (Ψ). It was mainly divided into three groups i.e. moving bed flow, dilute flow and plug flow. It was found that dilute phase is clearly visible in Jones (1990) diagram, which was not seen in basic bulk material diagram.

Pan (1999) developed a new flow mode diagram for the purpose of selecting suitable flow mode for a particular material by replacing particle density with "loose poured" density in Geldart classification diagram . Pan proposed that bulk solid material can be divided into three groups i.e. PC1 for fluidized dense phase flow, PC2 for plug flow, PC3 for dilute flow by simply measuring loose poured density and median particle diameter.

Pan utilized the same technique that Geldart used in determining A-B boundary by replacing particle density with loose poured density. The boundaries may be defined as follows:

Table 2.1: Boundaries for Pan's diagram

Boundary	**Pan diagram**
PC1-PC3	dp x ρ_{bl}= 0.1206
PC2-PC3	ρ_{bl} =1000

From this he concluded that material fall in PC1 category are excellent candidates for fluidized dense phase and can be transported gently from dilute to fluidized dense phase. Materials falling under PC3 category appeared to be dilute phase capable and PC2 category are plug flow capable.

Sanchez et al. (2003) developed a predictive model by measuring permeability and de-aeration time of various particles and related it to Geldart classification. Sanchez conducted a dimensionless analysis in two dimensional and three dimensional on various basic and air-particle characteristics.

It was found a better choice for representing the various parameters in three dimensional rather than two dimensional. The best correlation found in the study was using dimensionless number that are function of P*, de-aeration factor (Grt) ,minimum fluidization velocity (U_{mf}).

Diagram between P* and Grt was made with mode of the flow data which shows good predictive capabilities. The analysis also showed that materials, which do not fall into the clusters in line with their Geldart classification types are most likely due to secondary parameters (such as cohesion, moisture etc.) which can effect the flow modes of the materials.

Jones and Williams (2008) developed a new two dimensional diagram that could predict the three pneumatic conveying flow modes without the need to determine the de-aeration value. The diagram was plotted between loose poured density and permeability because of the difficulties faced for determining de-aeration factor. The boundaries in this diagram are empirical in nature which may change according to data available.

Table 2.2: Boundaries for Jones and William's diagram

Boundary	**Proposed diagram**
Fluidized Dense phase-Dilute phase	$\Psi\ \rho_{bl}{}^{3/4} = 300$
Dilute-Plug flow	$\Psi = 30\ X\ 10^{6}$

The characteristics were similar to the basic flow diagram for fluidized dense phase and plug type flow. In this diagram the dilute phase is clearly visible, which was difficult to be found in other diagram. The results obtained from this diagram also eliminated the confusion of de-aeration values defined by different researchers.

Baretta et al. (2007) developed a new rotational tester based on peschl test for the measurement of flow properties of aerated powders and compares the rheological properties of powder with aeration and without aeration. The test was carried on two powders magnesium carbonate and silica powder.

Incipient shear experiment conducted on both powders and it was found that the aeration does not affect the unconfined yield strength and its intrinsic rheological properties. With aeration pressure drop in gas partially balance the normal load acting on the particles so it only modify the normal state of stress. A dynamic shear experiment also shows same results.

Baretta et al. (2007) also carried out experiment on measurement of permeability which gives useful information on powder bed structure. It shows that powder with aeration along with shear deformation powder bed structure does not change relative to the case of static bed compacted by

shear deformation without aeration. The result shown by silica powder does not provide any conclusion.

Hirota et al. (2002) developed the relationship between the pressure drop in an inclined pipe and the mechanical properties of the powder. They have used the high density and low velocity pneumatic conveying of the powders (flyash, silica, soft flour) using cavity pump. They performed tests on various angles: 0,20,30,45,60,90 degrees. The dynamic internal friction factor was used for the calculation of a theoretical pressure drop per unit length of the pipe. From various relations, it was clear that pressure drop coefficient for powder conveying pipe can be obtained from dynamic internal friction factor and inclined angle of pipe. The value if $\lambda Fr/2$ change due powder friction factor however takes maximum value at 30- 45 degree of inclined pipe.

Rabinovich and Kalman (2011) developed a generalized flow regime diagram based on Reynolds number and Archimedes number for vertical pneumatic conveying and fluidized bed system. They carried out various experiments and study the influence various parameters such as pipe diameter and solid concentration on transition velocity in vertical pipe and they found that variation in column/pipe diameter does not affect the transition velocities. One of the most significant result was Geldart classification does not relate only to fluidized bed, but also to pneumatic conveying system. The boundaries in Geldart chart were replaced by modified Re and Ar power law relationship.

Leutria et al. (2014) compared traditional techniques to evaluate the characteristics of flow properties of cohesive powders with methodologies provided by FT4 Rheometer. Seven different materials ranging from nanoparticles to Geldart B powders were tested. In this study six different

methods i.e. shear cell test, consolidations test, aerated and tapped densities measurement, dynamic test, fluidization test and aeration test were employed to make the comparison to determine the theoretical relationship between them. These methods were also examined with regard to their ability to differentiate between different powders. The powder rheometer produces quick and repeatable measurement of data when the powder response to various conditions. The results showed that level of cohesiveness of powders have greater impact on the characterization techniques having different working ranges. It has been found that they were useful to compare similar materials rather than the discrimination of very different materials. The data obtained from different blade testing techniques almost same as which was obtained from traditional techniques.

Xu and Zhu (2006) investigated into the effect of mechanical vibration on fluidization behavior of fine particles. They studied a wide range of fine particles with average size varying from 4.8-216 μm including Aluminium oxide, glass beads, titanium oxide and calcium carbonate. They examined the role of vibration on fluidization of fine particles with respect to bed pressure drop, bed expansion ratio, agglomeration and tensile strength of bed materials. They found significant change in fluidization behavior of fine particles particularly for Geldart C type powder. The vibration leads to decrease the minimum fluidization velocity with higher pressure drop. The fluidizing quality of materials with vibrations depends on many factors such as Geldart type particles, particle size distribution, particle shape and also on vibration parameter (amplitude, frequency, angle) applied. They observed dramatically reduction in average size and segregation of agglomerates and also lower the tensile strength of materials when the fluidization was assisted with vibration.

Gupta et al. (2009) determined the minimum fluidization velocity of fine tailing materials such as zinc slime, iron-ore tailings, post and pre hydro-cyclone uranium tailings and fly ash. They carried out fluidization tests by using Plexiglas tube of diameter 150 mm and height of 600 mm. They compared the experimental values of minimum fluidization velocity with several correlations reported in literature. They found that most of the correlations to determine U_{mf} underestimated the experimental value of four tailing materials, whereas fly ash showed larger deviation. They also found that certain correlations predicted well for the four powders which belongs to Geldart group C as these correlation take into effect of inter-particle forces and degree of cohesiveness. The Colter and Rivas (2004) equation was modified to study the combined effect of particle size and density on U_{mf} and found that increase in particle size and density leads to increase in the value of minimum fluidization velocity.

Liu et al. (2015) examined the fluidization behavior of superfine particle (Silica) having mean diameter of 5.181μm. They conducted experiments in transparent glass tube having internal diameter of 50 mm and height of 2237 mm. In their study, they observed the fluidization behavior at different air velocities and found that the particles are fluidized in the form of agglomerates whose size was larger than primary particle size. The minimum fluidization velocity was determined with the help of fluidization curve drawn between pressure drop against superficial air velocity. the minimum fluidization velocity was found to be 3.4 cm/s. They conducted the bed collapse experiments to study the fluidization regime and quality. They have used 2D particle velocitimeter (PIV) to determine the agglomerate size distribution. They compared the agglomerate fluidization regime and particle size distribution of micro-particles with nano- particles and found the similar results between them. The agglomerate size distribution was found to be similar to Gaussian distribution. They measured the minimum

agglomerate diameter under the effect of Vander -wall cohesive force which was found to be 133 µm. They also suggested that due to very high agglomerate voidage of 0.966, it may have significant effect on the interaction between the agglomerate phase and gas.

2.7 Models for minimum fluidization velocity

Vasconcelos and Mesquita (2011) examined the minimum and full fluidization velocities of alumina fluoride of four different mean particle sizes which could be used to imagine the state of art round non metallic air fluidized conveyer of multiple outlets. They have used two different permeameters one rectangular and other circular made of acrylic sheets to visually observe the fluidization behavior of particles. They compared the experimental values obtained from fluidization curves with several correlations reported in literature. It was found that value of U_{mf} for d_p = 70.6 µm as predicted by Colter and Rivas (2004) and Vasconcelos (2011) were found in good agreement with experimental values with error less than 0.5 %. They also proposed the correlation to find the $U_{mf.}$

$$U_{mf} = 0.21(Ar)^{0.25} \frac{(\varphi_s)^{0.7}}{(1.05\ \varepsilon_{mf})^{0.7}} (d_{50}\ g)^{0.5} \qquad (2.2)$$

Xu and Zhu (2008) developed a new correlation for finding minimum fluidization velocity for fine particles. They modified the Ergun (1949) equation of pressure drop for packed bed and equalized the forces during fluidization by taking the effect of interparticle forces acting between them. Based on previous experimental data available in the literature they proposed a relationship between voidage at minimum fluidization (ε_{mf}) and the particle size. They introduced two new constants in the new relation, first was E_G, which represents the

gravitational force effect and the second was E_C, which represents the cohesive force effect. They employed the previous experimental data from Xu and Zhu (2006) into their new derived correlation and compared with existing correlations of Leva (1959) and Wen and Yu (1966). They found that each of the correlation show different degrees of agreement depending on particle size. They also found satisfactorily results for particles belong to Geldart group A,B,D,A/C from the prediction made by new correlation. Their model is given by equations 2.3.1 to 2.3.4.

$$Re_{mf}^2 + \frac{85.71(1-\varepsilon_{mf})}{\varphi_s} Re_{mf} = E_G + E_C \quad (2.3.1)$$

$$E_G = 0.57\, \varphi_s\, \varepsilon_{mf}^3 Ar \quad (2.3.2)$$

$$E_C = 4.79 * 10^{-9} \frac{\varphi_s\, \varepsilon_{mf}^{0.52} \rho_g d_{50}}{L_o\, \mu_g^2} \quad (2.3.3)$$

$$\varepsilon_{mf} = 0.77(d_{50} * 10^{-6})^{-0.124} \quad (2.3.4)$$

Abrahamsen and Geldart (1980) examined the effect of gas on powder behavior in fluidizing column. They have used cylindrical fluidization column of internal diameter 0.15 m made of prepex material for carrying out the fluidization experiments. The experimental conditions were ambient conditions. A probe was used to measure the bed pressure drop. They have used 23 different powders with mean size varying from 20μm to 72μm and with particle density between 1100 to 4600 kg/m^3. They observed that powder belonging to group A category shows good fluidizing characteristics with air but when interacted with hydrogen under same experimental conditions behave like group B powders with bubbling/slugging.They found equation (2.4) provides good prediction for finding minimum fluidization velocity on their fine powders.

$$U_{mf} = \frac{0.009\left(\rho_s - \rho_g\right)^{0.934} g^{0.934}\, d_{50}^{1.8}}{\mu_g^{0.87} \rho_g^{0.066}} \quad (2.4)$$

Wen and Yu (1966) proposed a relationship between two dimensionless number i.e Reynolds number and Archimedes number to determine the minimum fluidization velocity in which no relationship of ε_{mf} and φ_s was required. They have developed the correlation based on the well known Ergun equation for fixed bed pressure drop. They have validated their model with available literature data and found a standard deviation of 34% and ±25% average deviation from their correlation. The model shows greater accuracy with respect to others models of minimum fluidization velocity. The model also covers the widest range of Reynolds number ($0.001 < Re_{mf} < 4000$).

$$U_{mf} = \frac{\mu_g}{\rho_g\, d_{50}} \{ 1135.7 + 0.0408\, Ar)^{0.5} - 33.7 \quad (2.5)$$

Xie and Geldart (1995) studied the effect of temperature and gases on U_{mf} and U_{mb} on 12 different FCC powders having particle size varying from 26 µm to 137 µm. They performed experiments by using fluidizing column of diameter of 0.152 m which consists of two different parts. The bottom part was made up of stainless steel and having height of 0.6 m. Three tapping were installed along the height of column to determine the temperature. The top part having height 0.4 m was made with the top section open. They found that gas absorption in FCC powders have considerable effect on fluidizing behavior. They modified the Abhramsen and Geldart (1980) equation for finding minimum bubbling velocity and suggest that their correlation can be used to predict U_{mb} of FCC powders up to 500 C with ±20% accuracy. They also found that with the rise in temperature the minimum fluidization velocity decreases. They

experimentally determined the minimum fluidization velocity and validated by the following correlation:

$$U_{mf} = \frac{\varepsilon_{mf}^3}{1-\varepsilon_{mf}} \frac{(\rho_s - \rho_g)\, g\, d_{50}^2}{180\, \mu_g} \tag{2.6}$$

CHAPTER 3: TEST FACILITY AND EXPERIMENTAL PROCEDURES

3.1 Test facility for fluidization and de-aeration

A test facility was developed at the Laboratory for Particle and Bulk Solid Technologies, Thapar University for carrying out fluidization and de-aeration testing. A schematic of test facility for fluidization and de-aeration is shown in Figure 3.1.

Major components of the apparatus are as follows:-

- Blower with max pressure of 160 mbar
- Variable frequency drive
- Two Rotameters
- Air plenum chamber
- Fluidization column of internal diameter of 1 m
- U-Tube manometers

A side channel centrifugal type blower (1 H.P and Maximum air delivery of 145 m^3/hr) was used to supply air. A variable frequency drive was attached to the blower to control the air flow rate by changing the frequency, i.e. controlling the RPM of the blower. Two rotameters were installed in parallel in the air line to measure the air flow rate in appropriate range of flow. The regulating valves were installed in the air pipeline to obtain different air flow. A mild steel plenum chamber of internal diameter of 102 mm and height of 150 mm was attached to the fluidization column for uniform distribution of air. A porous membrane or filter (5 µm mesh size) was placed between the plenum chamber and fluidizing column for supporting the material (powder). This also functions as air distributor. Fluidizing column of internal diameter 102 mm and height of 1 meter was attached in vertical position above the plenum chamber as shown in Figure 3.1. The column was made of acrylic tube for clear

visibility of the fluidizing behavior of powders. Five pressure tappings were installed at equal distances from each other along the height of the column for the measurement of pressure drop across the bed material. Each pressure tapping was attached with two more taps installed along the circumference of the column in order to avoid disturbances during recording of pressure data in case one of the tapping gets clogged. The bed height was measured by attaching a centimeter scale on the column. The manometers were used to measure the pressure from each tapping. A high speed camera having speed of capturing of 60 frames per second was used to visualize the fluidization and de-aeration behavior of powders.

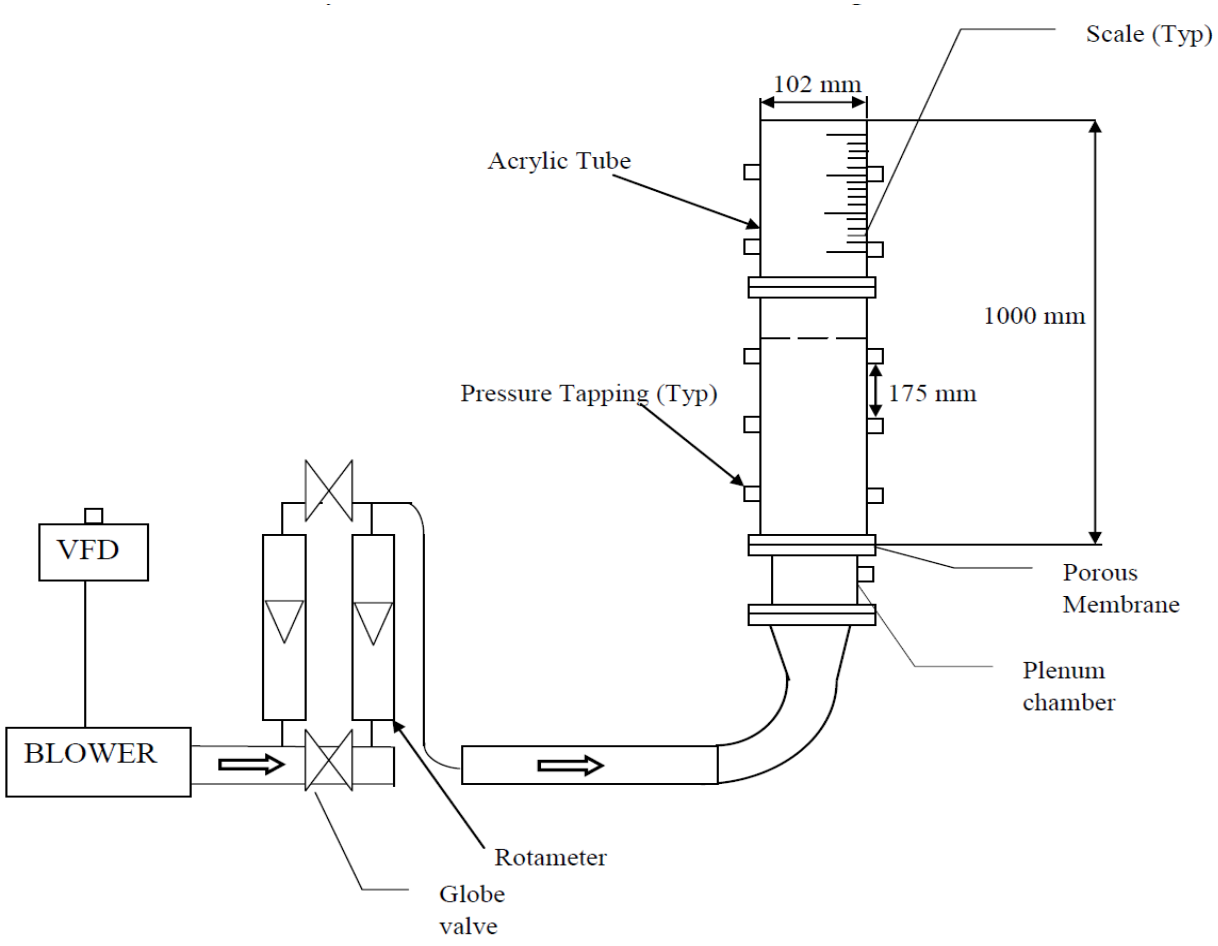

Figure 3.1: Fluidization and de-aeration Chamber

3.1.2 Physical properties of test products

Table 1 gives the key physical properties of different fly ash samples. For analysis seven different fly ash samples were collected from the same field of different ESP hopper. The bulk density and particle density was measured by standard methods for each sample. The variation of particle density for different samples of fly ash is between 2014 – 2032 kg / m^3 and the variation of bulk density is between 759 – 848 kg / m^3 being 759 kg / m^3 for fine fly ash and 848 kg / m^3 for coarser fly ash. However, the values of poured bulk density having an error (±10%) due to points from which samples were taken.

Table 3.1: Physical properties of different fly ash tested

Sr.no.	**Material tested**	**d_{10} (µm)**	**d_{50} (µm)**	**d_{90} (µm)**	**ρ_s (kg/m^3)**	**ρ_b (kg/m^3)**
1	Fly ash from ESP Hopper 1	42	139	316	2015	848
2	Fly ash from ESP Hopper 2	23	102	235	2014	839
3	Fly ash from ESP Hopper 3	23	97	213	2018	830
4	Fly ash from ESP Hopper 4	18	69	170	2025	818
5	Fly ash from ESP Hopper 5	14	53	141	2032	804
6	Fly ash from ESP Hopper 6	12	41	108	2030	780
7	Fly ash from ESP Hopper 7	6	21	63	2025	759

3.2.2 Calibration

A standard procedure is employed for the calibration of test column. Before starting the calibration ensure the whole test column is properly fitted and with no leakage of air from any of the points. Then all the pressure tapping are attached to the manometers and air is blown into the test column with the help of a blower and then manometer readings are checked to ensure that all the manometer readings should come same.

3.2 Operating procedure

Start up

1. Switch on the power supply and check the display of the VFD.
2. Connect the manometers to the experimental system using the connections provided. Fix all the flexible pipes at the designated points.
3. Start the blower with the help of run button on VFD and check that it is functioning properly.

Shut down

1. Fully close the regulating valves.
2. Turn off the blower with the help of stop button on VFD.
3. Turn Off the power supply.
4. Plug out all the pipes from the fluidizing column then remove the testing particles by unbolt the nuts from bottom side of column and clean the vessel with the help of compressed air.

Fluidization testing

1. Pour the testing product of known mass into the acrylic tube and note down the initial bed height.
2. The frequency of the blower was set up with the help of VFD in order to get a specific flow rate at a certain pressure.
3. Increase the air flow rate in small increments with help of regulating valves.
4. Continuously note down air flow rate and corresponding pressure with the help of the manometer.
5. Continue the measurement up to the maximum flow and then decrease the air flow rate again to note down the air flow rate and pressure data.
6. Repeat steps 1 through 5.

De-aeration testing

1. De-aeration testing can be done while doing the fluidization testing.
2. Increase the air flow rate up to fully fluidized state and run the system continuously for 3-4 minutes
3. Then air supply is cut off with the help of stop button of the VFD.
4. Record the pressure drop and the bed height with the help of high speed camera.
5. Plot the graph between pressure drop per unit length and time.
6. Plot the graph between bed height against time

3.3 Scanning electron microscope (SEM)

A high energy beam of electrons is made incident on the sample to produce the scanned image of the particles. These energetic electrons then interact with the atoms of the sample and produce different signals that are detected by the sensors.

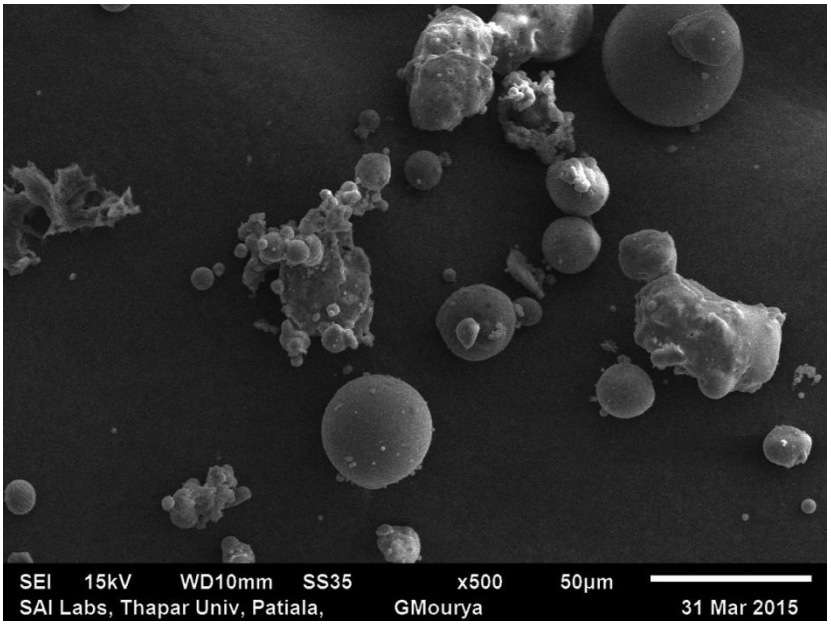

Figure 3.2: Microscope image of fly ash 1 (median particle size 139 µm)

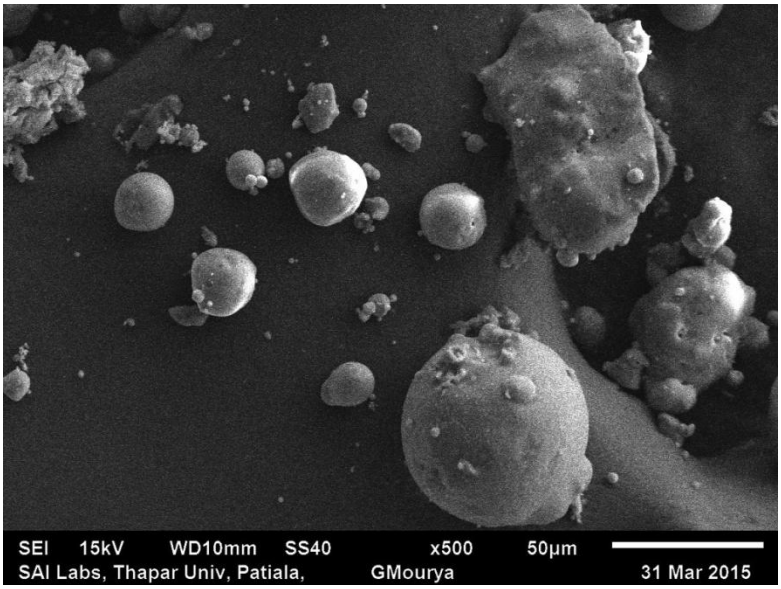

Figure 3.3: Microscope image of fly ash 2 (median particle size 102 µm)

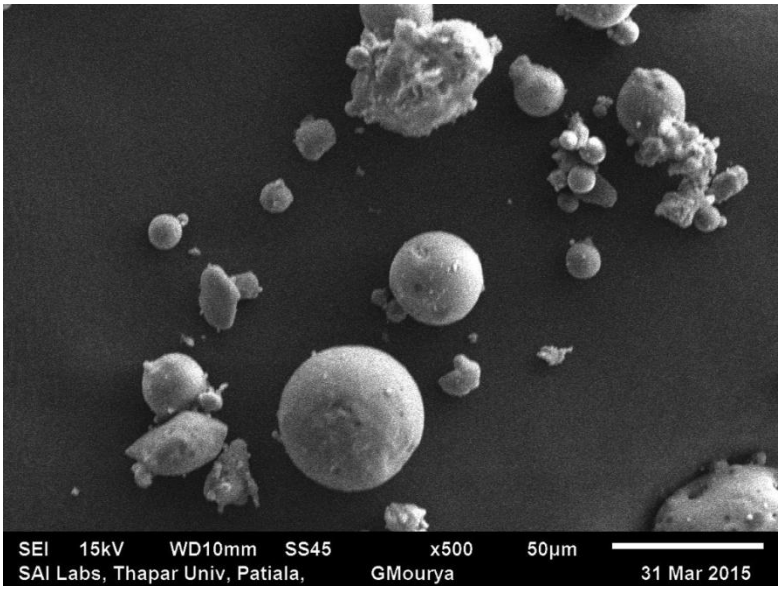

Figure 3.4: Microscope image of fly ash 3 (median particle size 69 µm)

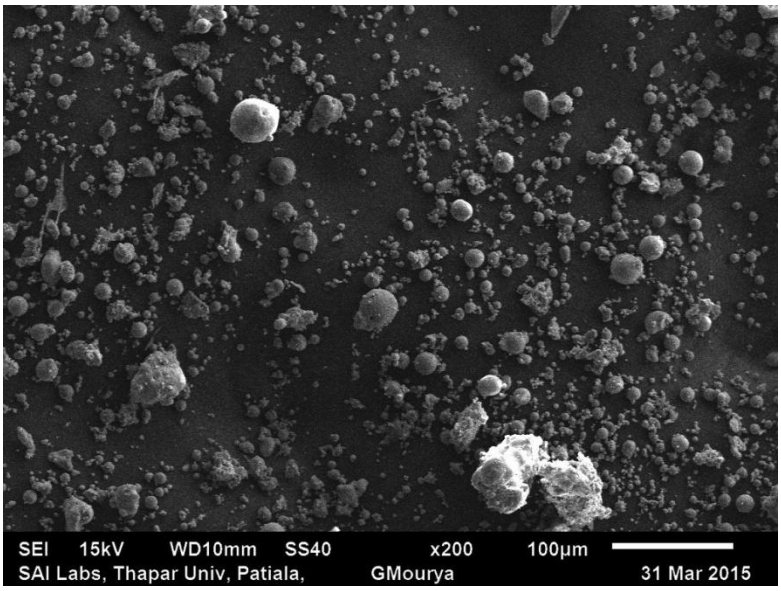

Figure 3.5: Microscope image of powder 4 (median particle size 21 µm)

The equipment used was SEM-JSM-6510LV JEOL.The shapes of particles were determined with the help microscopic images obtained from SEM. It shows that the shape of particles is almost spherical. So the sphericity can be taken as 1.

3.4 Particle size distribution (PSD)

Particle size analysis was done using laser diffraction analyzer (Malvern, Mastersizer 2000).

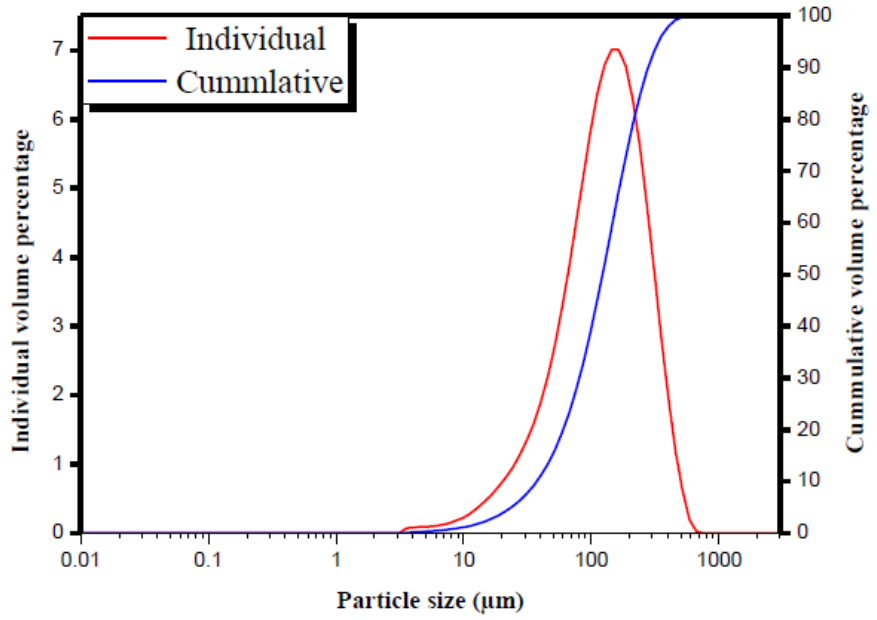

Figure 3.6: Particle size distribution of fly ash 1

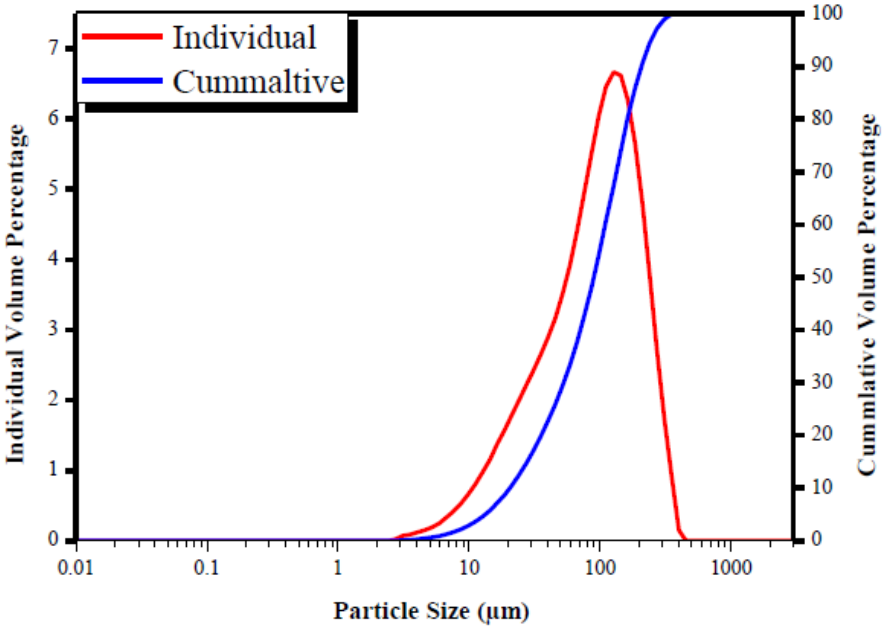

Figure 3.7: Particle size distribution of fly ash 2

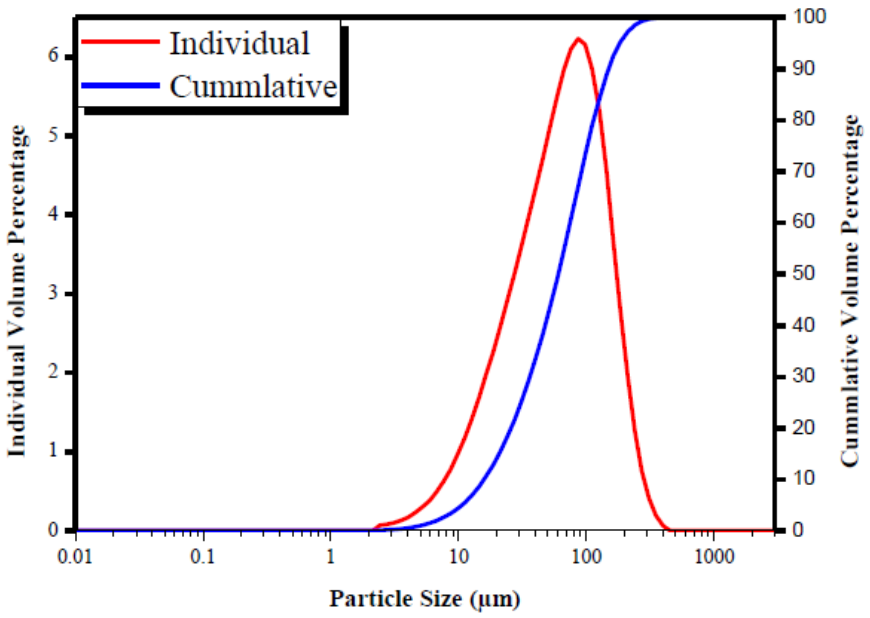

Figure 3.8: Particle size distribution of fly ash 4

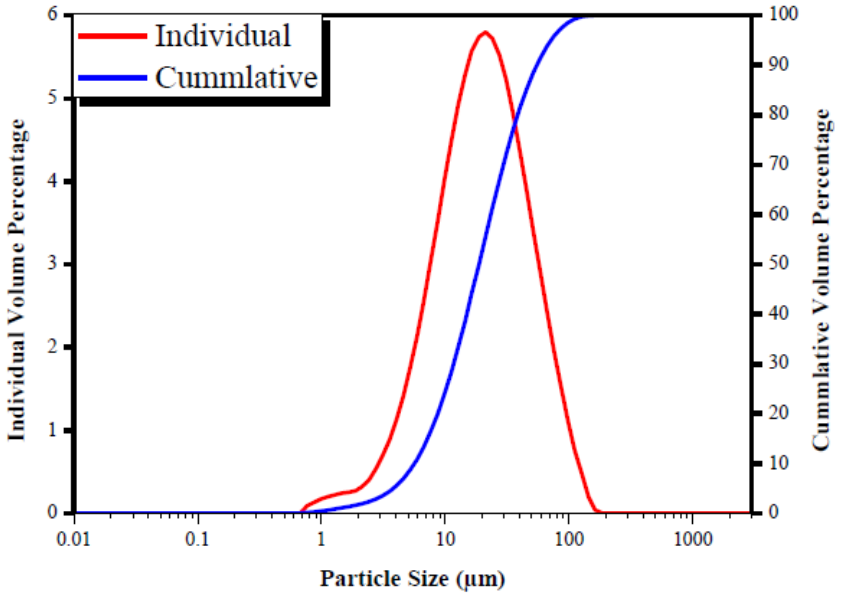

Figure 3.9: Particle size distribution of fly ash 7

Figure 3.6 to 3.9 shows the particle size distribution of fly ash 1,2,4 and 7. The red line in the figure 3.6 to 3.9 shows individual volume percentage, whereas the blue line represents the cummlative volume percentage.

CHAPTER 4: RESULTS OF FLUIDIZATION AND DE-AERATION

4.1 Fluidization testing

The fluidization characteristics of powders were studied by measuring the pressure drop per unit length at different fluidization velocity. The most important and fundamental parameter in designing the fluidized bed is the minimum fluidization velocity, which shows the transition from packed bed to fluidized bed. It can be determined by plotting the ideal fluidization trend line of bed pressure drop versus superficial air velocity, pressure drop increasing linearly against velocity in ideal condition and another linear trend parallel to X-axis at constant pressure drop. The velocity U_{mf} was defined as the intersection of these two trend lines. This method is adopted as per Xu and Zhu (2006) and Liu et al. (2015). The fluidization behavior of fly ash 1 is depicted in Figure 4.1. During the fluidization of fly ash 1 (median particle size of 139 μm), small bed expansion was observed during the initial stage. When the velocity of air was further increased bubbling occurred at the top of the bed. Further increase in air flow led to formation large bubbles resulted in fully fluidization state. The highly concentrated bed was observed at the bottom of the column during fully fluidization state. Larger pressure drop per unit length (about 5.6 kPa/m) was seen and the minimum fluidization velocity was 0.0285 m/s. Also the bed got expanded almost 1.2 times the initial height at fully fluidized state. There is gradual change of pressure drop with increasing air velocity with larger radius of curvature as seen in figure 4.1 for fly ash 1 due to wide particle size distribution (see Table 3.1).

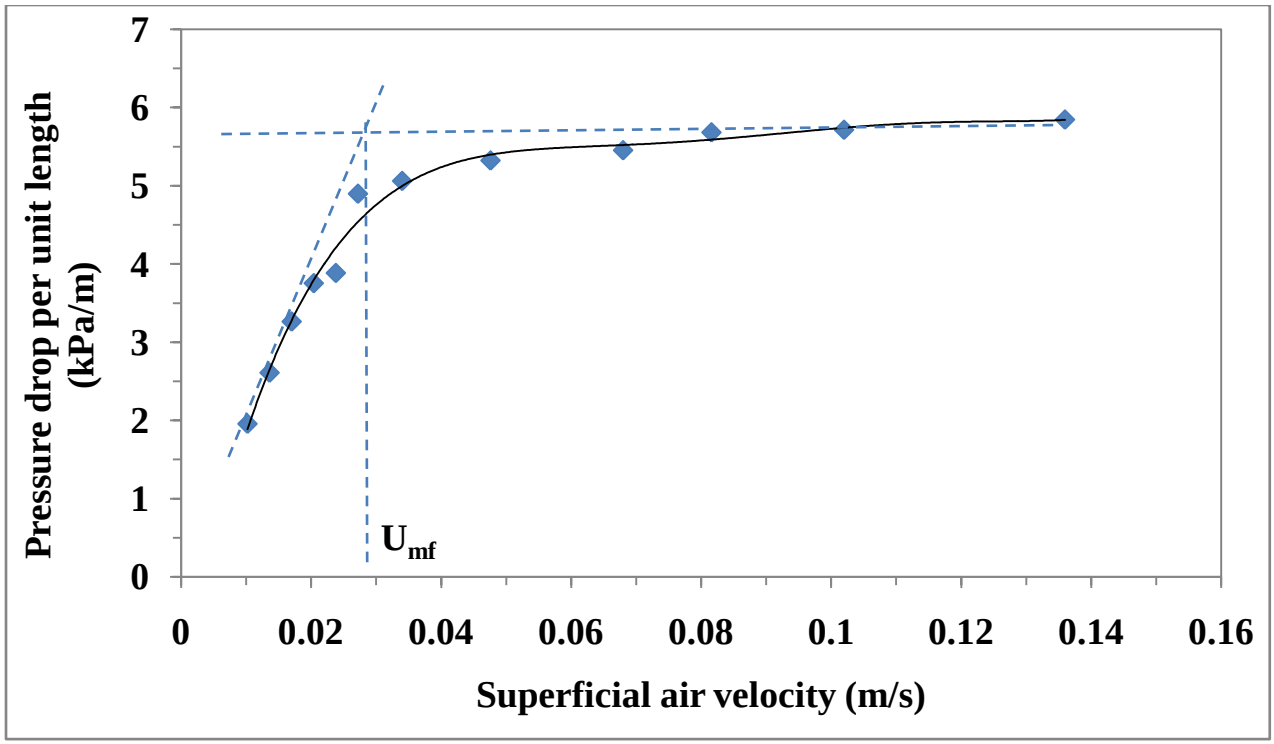

Figure 4.1: Pressure drop per unit length versus superficial air velocity of fly ash 1 during fluidization

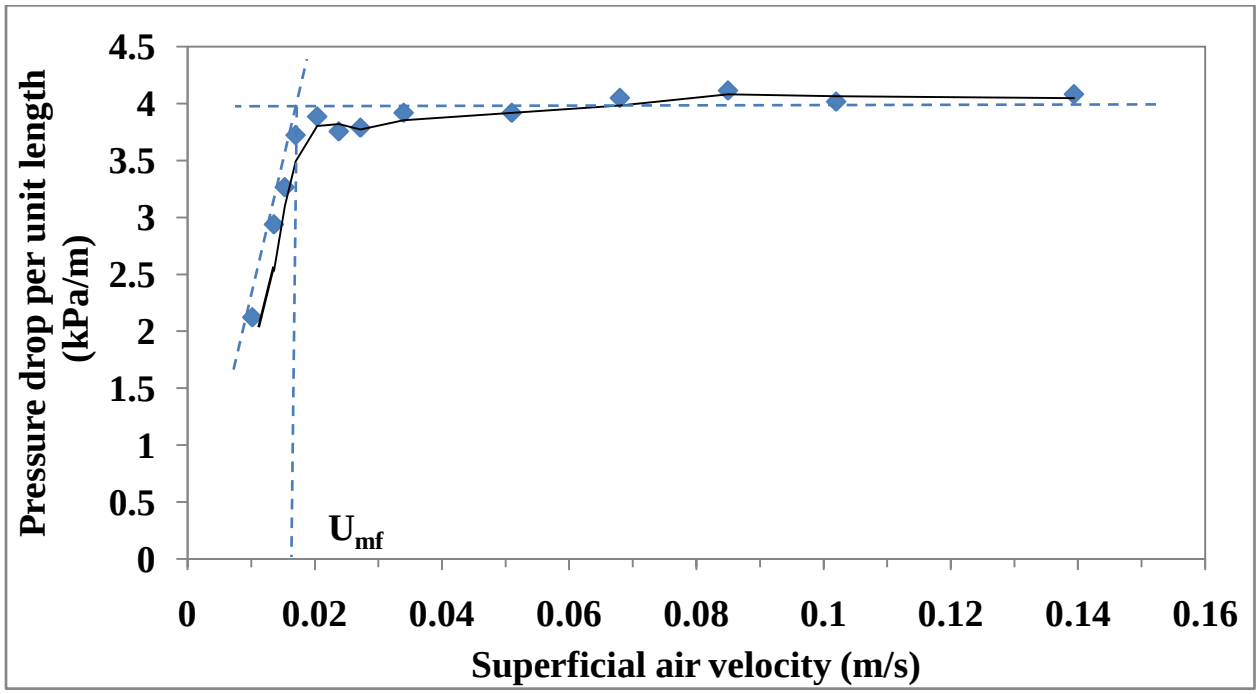

Figure 4.2: Pressure drop per unit length versus superficial air velocity of fly ash 2 during fluidization

The pressure drop per unit length was smaller than fly ash 1. Figure 4.2 elucidate the variation of pressure drop per unit length against the superficial air velocity of fly ash 2. The minimum fluidization velocity was measured by same the procedure as explained above for fly ash 1. Intially when the air flow was increased in small amount then there was little bed expansion. Further increase in the air flow rate led to formation of stable bubbles observed at top of the bed. Then the velocity of air was increased to obtain fully fluidization state. Lower minimum fluidization velocity of 0.016 m/s was seen than fly ash 1 due to smaller particle size. Fig 4.2 show that there is sharp change in pressure drop with increasing air velocity with respect to fly ash 1. The reason for this sharp transition in trend is due to narrow particle size distribution as compared to fly ash 1.

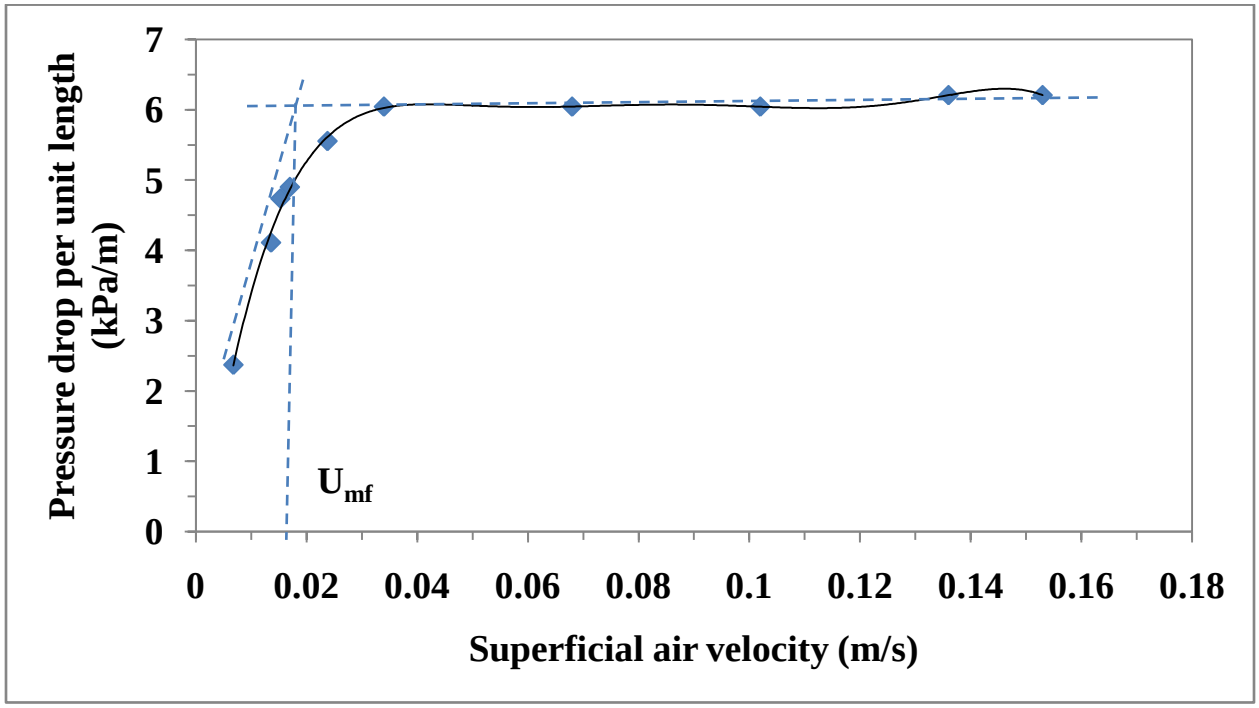

Figure 4.3: Pressure drop per unit length versus superficial air velocity of fly ash 3 during fluidization

Figure 4.3 shows the fluidization curve for fly ash 3 having a median particle size of 97 µm. Larger bed expansion was observed when the air flow was increased in small proportion when compared to fly ash 1 and 2. Small bubbles were clearly seen at the top of the bed. The fully fluidization state was obtained by increasing the air flow rate beyond minimum fluidization velocity. The pressure gradient at fully fluidized state was found to be larger and its value is 6.1 kPa/m. The minimum fluidization velocity as obtained from fluidization curve was 0.018 m/s.

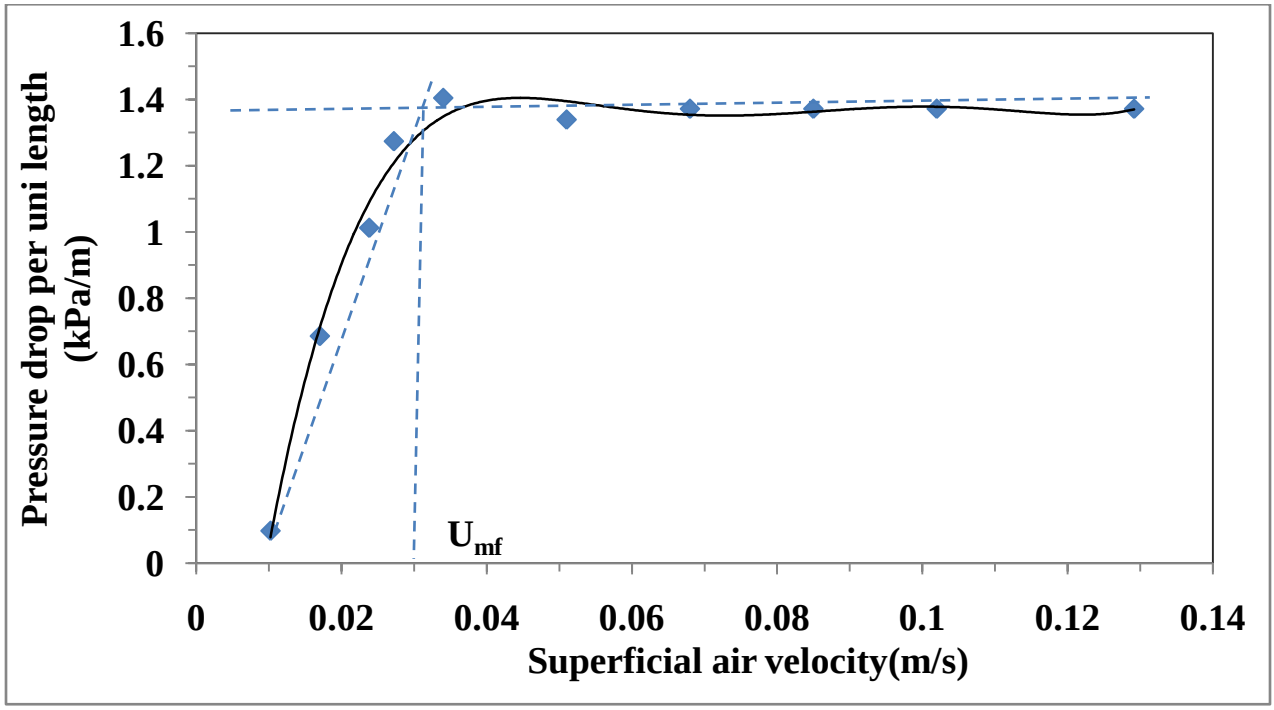

Figure 4.4: Pressure drop per unit length versus superficial air velocity of fly ash 4 during fluidization

Figure 4.4 shows the fluidization characteristics of fly ash 4 (median particle size of 69 µm). The bed expansion of fly ash 3 was larger as compared to fly ash 1,2 and 3. The fluidization took place in a turbulent manner. During the fully fluidization state, the fines leave the bed due to high gas velocity. Smaller pressure drop per unit length of 1.4 kPa/m was seen as compared to fly ash 1,2 and 3. The minimum fluidization velocity as measured from figure 3 was larger than

fly ash 3 and its value is 0.03 m/s. The reason for high fluidization velocity of fly ash 4 could be the fines leaving the bed at high air velocity.

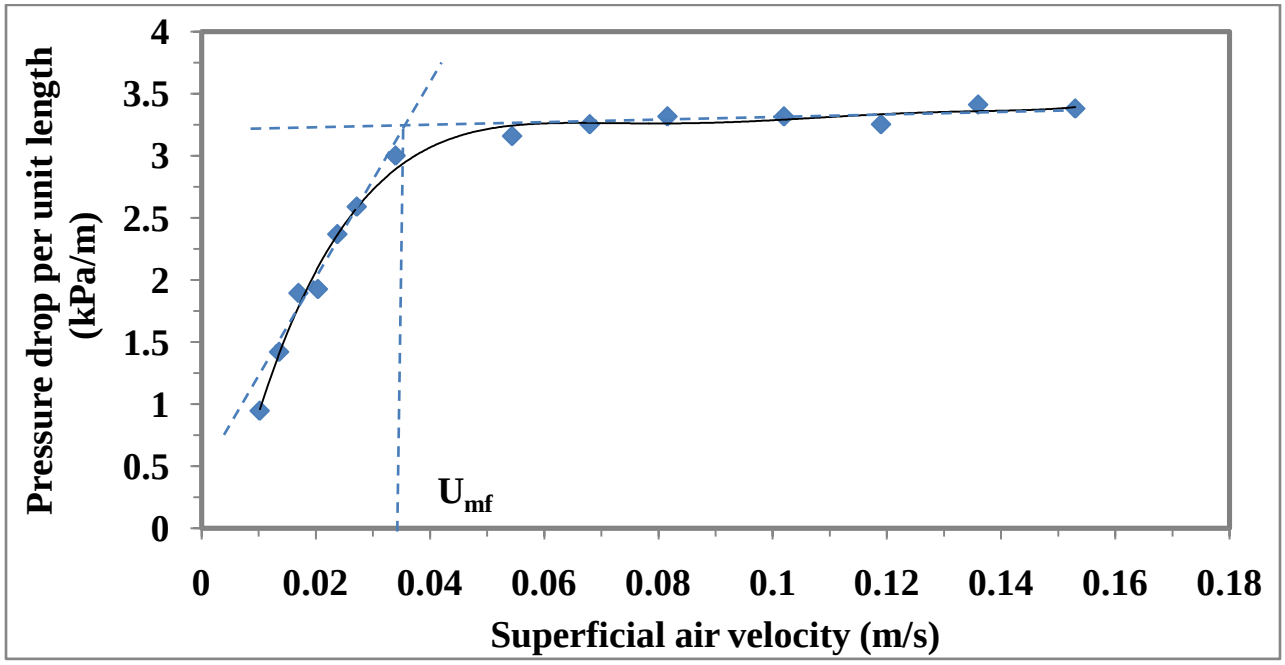

Figure 4.5: Pressure drop per unit length versus superficial air velocity of fly ash 5 during fluidization

Figure 4.5 shows the variation of pressure drop per unit length plotted against superficial air velocity of fly ash 5 (median particle size 53µm). The larger bed expansion was observed as compared to fly ash 4. During fluidization, the particles tend to coat the inner surface of fluidizing column which leads to difficulty in measuring the bed height. The fully fluidization pressure drop per unit length was found to 3.4 kPa/m which was larger as compared to fly ash 4. The minimum fluidization velocity as measured from figure 4.5 was 0.036 m/s.

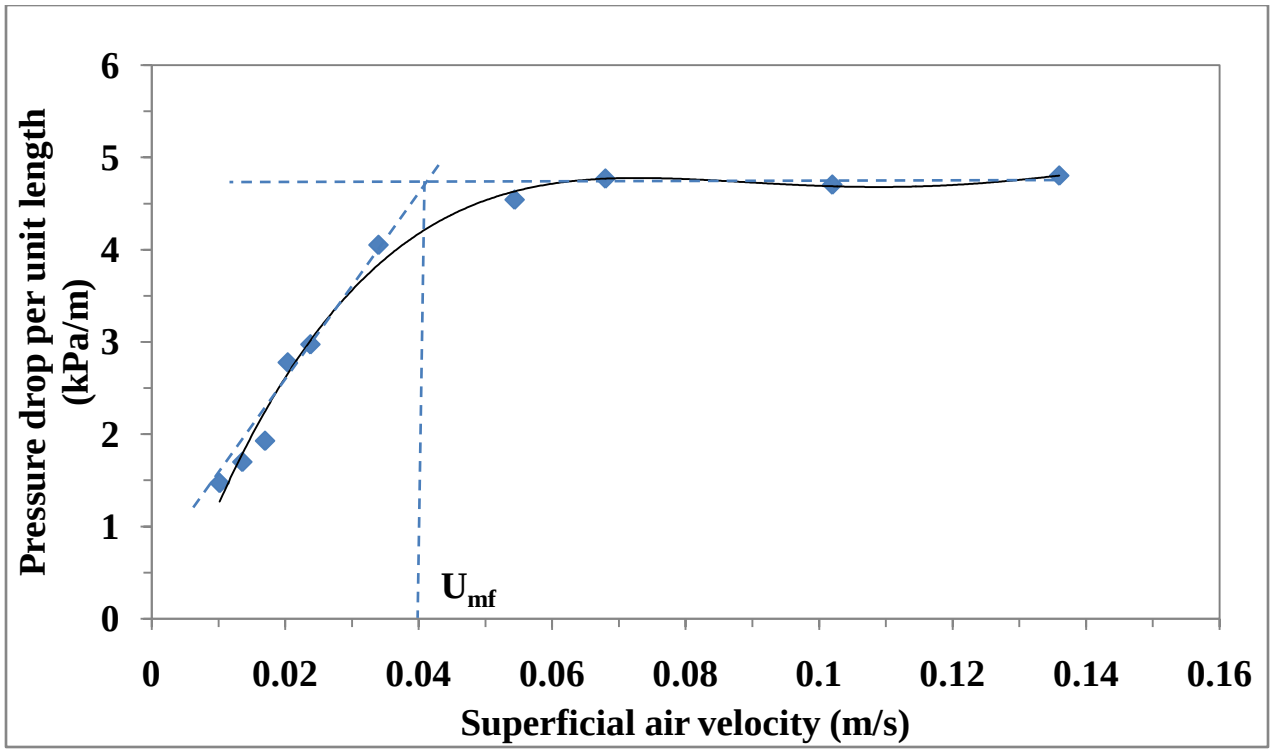

Figure 4.6: Pressure drop per unit length versus superficial air velocity of fly ash 6 during fluidization

Figure 4.6 represents the fluidization behavior of fly ash 6 having median particle diameter of 41 µm. During the initial stage when the air was increased in small proportion there was no change in initial bed height. When the air velocity reached the 0.02 m/s channeling occurred which led to partial fluidize the material. After channeling, a little increase in air velocity leads to the whole bed got lifted as a plug due to strong Vander wall forces acting between particles. When the air velocity was increased beyond minimum fluidization velocity, the fluidization took place in a disorderly manner. The steady state pressure drop per unit length was found to be 4.7 kPa/m and minimum fluidization velocity was 0.04 m/s as measured from figure 4.6.

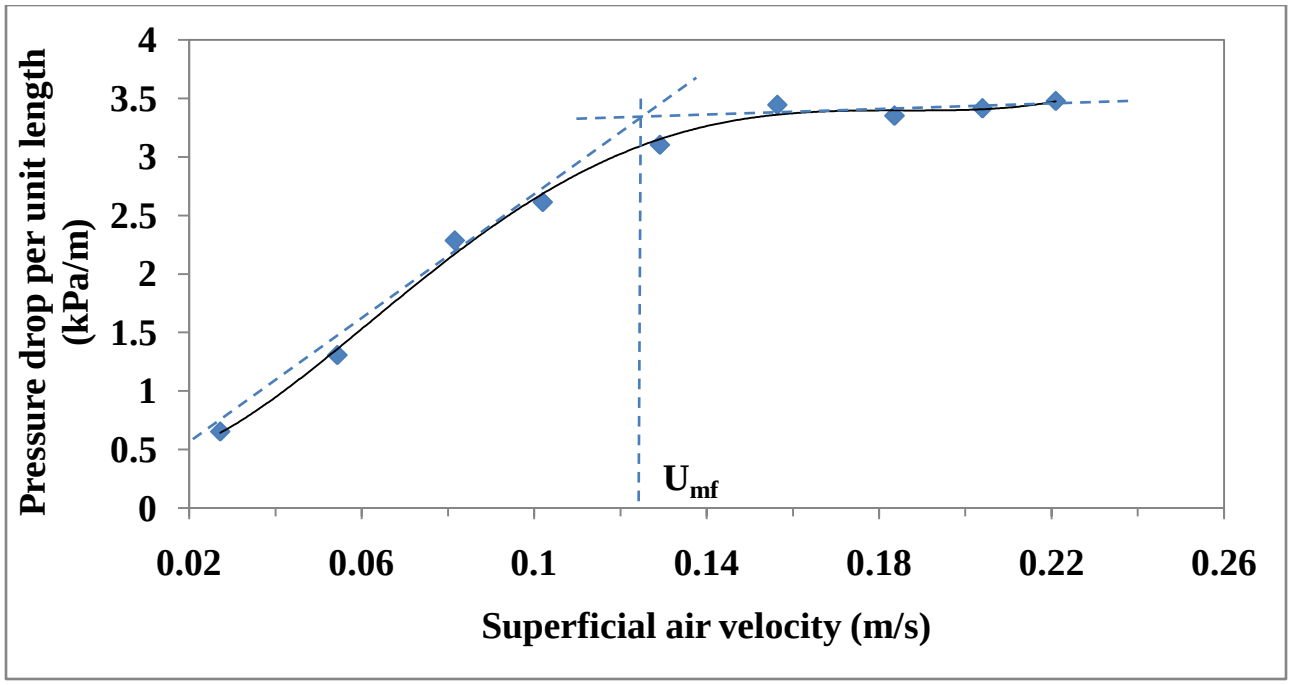

Figure 4.7: Pressure drop per unit length versus superficial air velocity of fly ash 7 during fluidization

For the fly ash 7 (median particle size of 21 µm) which belongs to Geldart C category, when the air flow is initially turned on and after increasing the air velocity in small proportion up to 0.03m/s, no fluidization of particles was observed in the column. Channeling occurred when gas velocity is in the range of 0.03-0.06 m/s which led to partly fluidize the particles .When the air velocity was further increased beyond 0.06 m/s, the whole bed got lifted off as a plug due to the strong inter-particle forces contributed by ultrafine particles. The fluidization of powders took place in the form agglomerates whose size is larger than median size particle due to cohesive nature of powders (Liu et al. 2015). During the fluidization of group C powders, Vander-wall forces dominates against the fluid force acting on particles,thus requiring high fluidization velocity for powders (Geldart, 1973). Figure 4.7 shows plot of pressure drop per unit length against the superficial air velocity. The measured minimum fluidization velocity for fly ash 7

from Figure 4.7 was 0.122 m/s. The steady state pressure drop per unit length was found to be 3.5 kPa/m.

4.2.2 Permeabiilty factor

Permeability factor was obtained by measuring the slope of the fluidization curve and taking the inverse of the slope. Table 1 shows the permeability factor obtained for different fly ash samples.

Table 4.1: Permeability Factor

Sr.No.	**Sample**	**Permeability Factor (m^2/kPa-s)**
1	Fly ash 1	0.005782
2	Fly ash 2	0.004248
3	Fly ash 3	0.004033
4	Fly ash 4	0.018214
5	Fly ash 5	0.011214
6	Fly ash 6	0.009221
7	Fly ash 7	0.041632

The permeability factor for fly ash 7 shows the higher value whereas for fly ash 3 it shows lowest value. The Mainwaring (1987) classification suggests that the material with high permeability factor shows plug mode of dense phase, whereas lower value of permeability factor value shows moving bed flow. Here, fly ash 7 shows the plug mode of flow with having higher permeability factor as compared to other fly ash.

4.2 De-aeration testing

De-aeration characteristics of powders were determined by recording the bed height or pressure variation with respect to time. It was clearly evident from the experiments that powders having smaller particle size were able to retain air for longer time as compared to powders having larger particle size.

After turning off the air supply, fly ash 1 and 2 showed drastic change(quick drop) in bed height as bed collapsed very fast due to larger particle size then the bed got compacted under the effect of gravity leading to fast de-aeration. Figure 4.8 and 4.9 show that air retention capability of fly ash 2 was larger than fly ash 1 because of smaller size of fly ash 2.

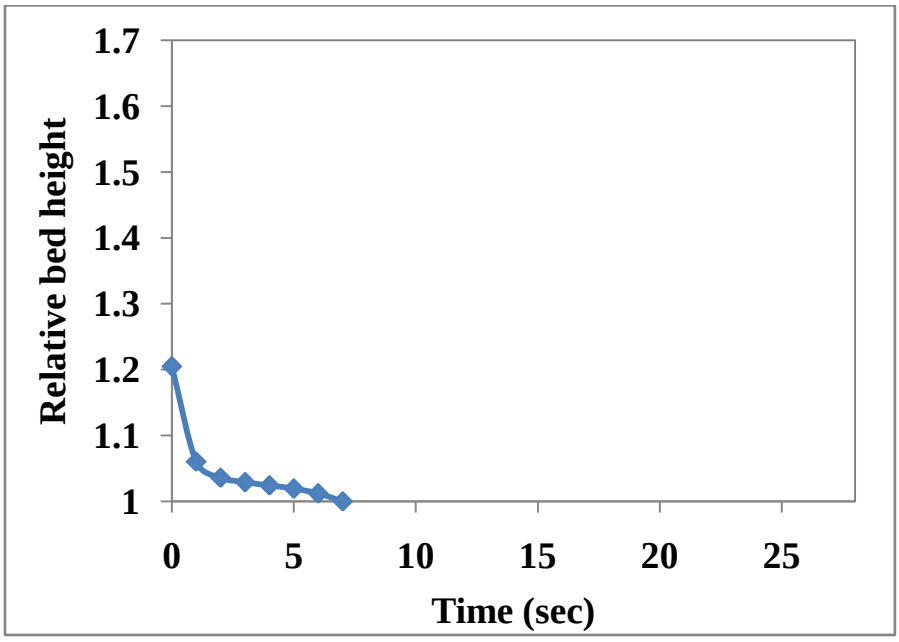

Figure 4.8: Drop in relative bed height vs. time for fly ash 1

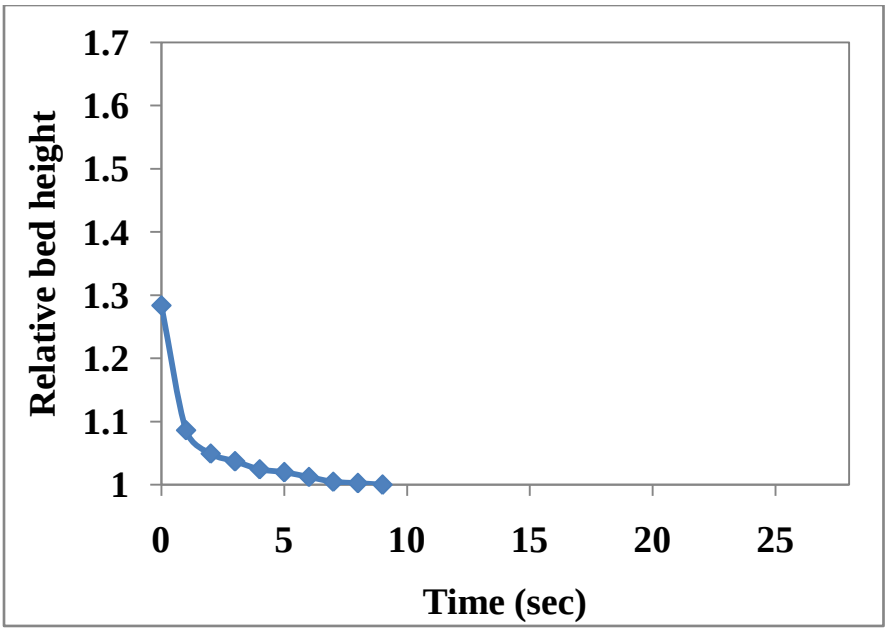

Figure 4.9: Drop in relative bed height vs. time for fly ash 2

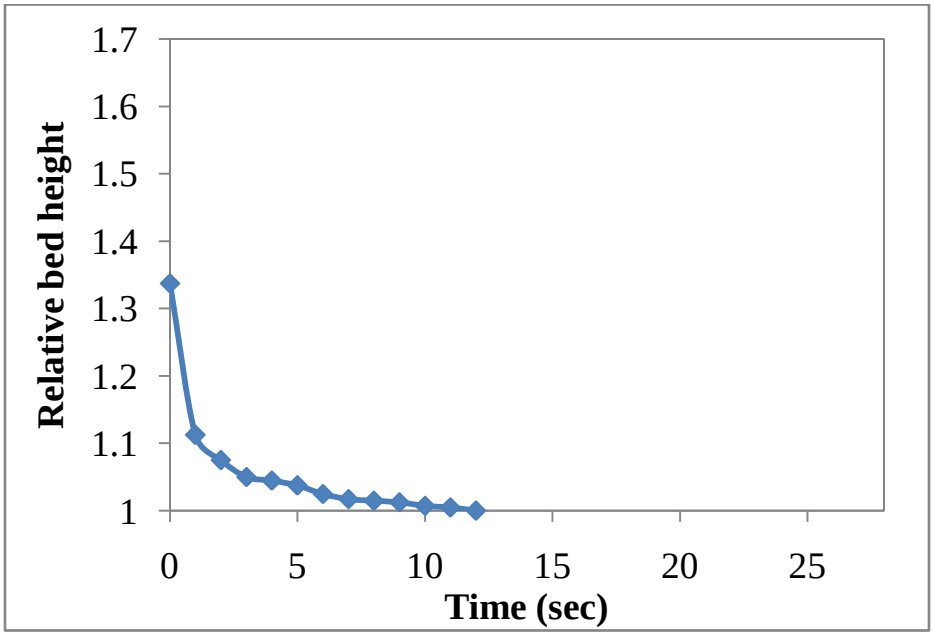

Figure 4.10: Drop in relative bed height vs. time for fly ash 3

Figure 4.10 depicts the de-aeration characteristics of fly ash 3. During the initial stage, the bed height shows severe change, then material got compressed under its own weight. Figure 4.10 clearly shows that the material de-aerate rapidly, but fly ash 3 holds the air for much longer time than fly ash 1 and 2.

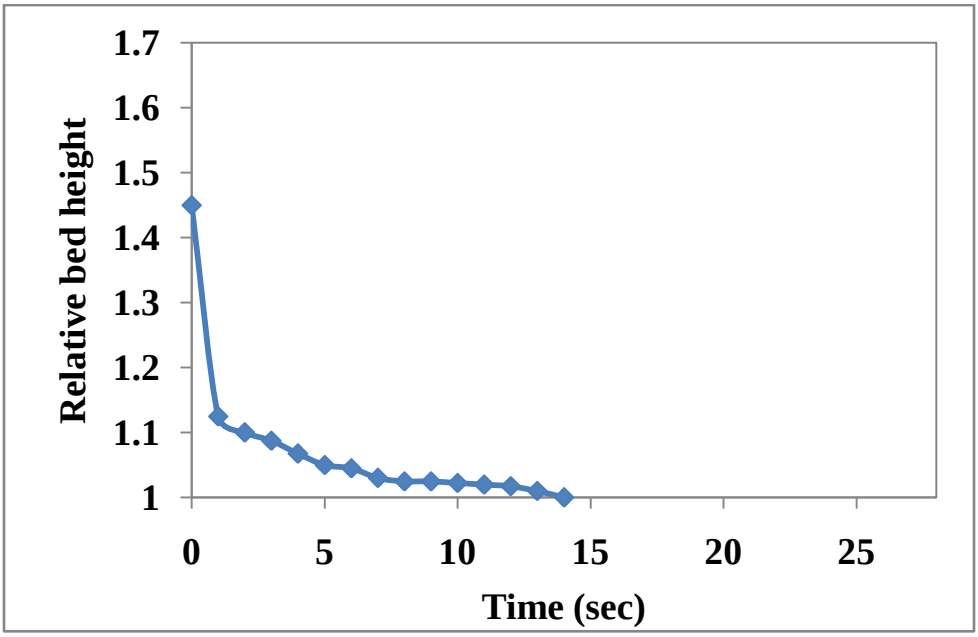

Figure 4.11: Drop in relative bed height vs. time for fly ash 4

Figure 4.11 represents the variation of relative bed height with time. Powder 3 shows that during the initial stage, the bed collapsed very fast as the large gas bubbles flew out of the bed first. Then relative bed height decreases gradually from 1.125 to 1.03 for 7 seconds, thereafter bed height reduced very slowly under the influence of gravity. This type of behavior was observed by typically Geldart A particles.

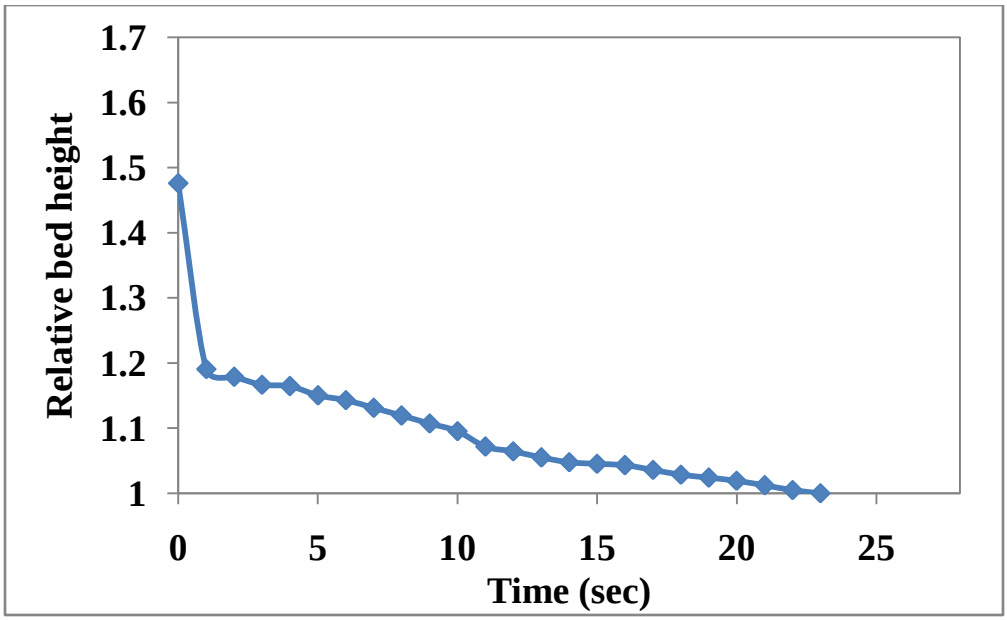

Figure 4.12 : Drop in relative bed height vs. time for fly ash 5

Figure 4.12 shows the plot between relative bed height and time for fly ash 5. When the air supply was turned off suddenly, the decrease in relative bed height occurred very fast. After few seconds, the stalled settling stage appeared which depicts the change in bed height occurred gradually for 11 seconds.Further to this, bed slowly comes to its initial position.

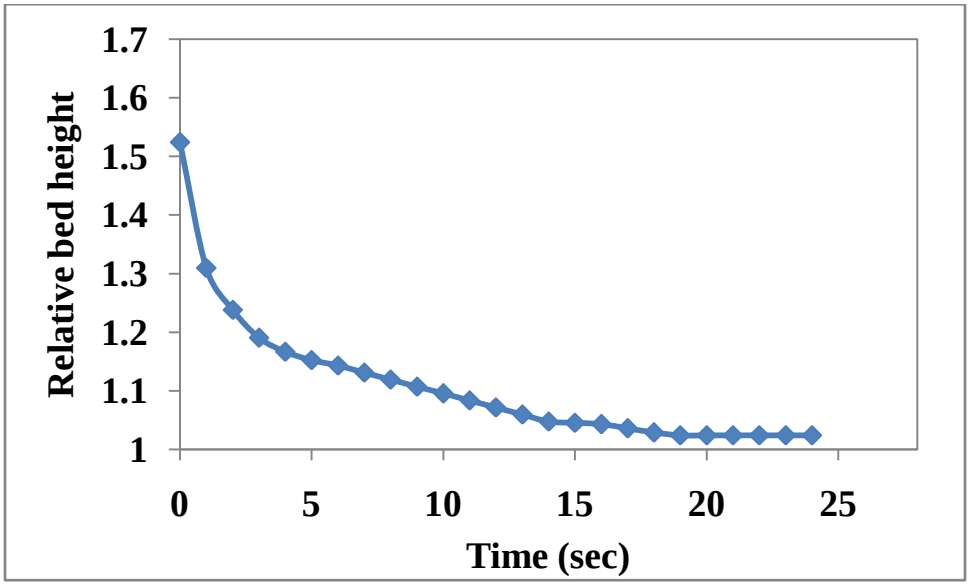

Figure 4.13 : Drop in relative bed height vs. time for fly ash 6

Figure 4.13 reveals de-aeration relative bed height variation for fly ash 6. It shows that fly ash 6 have good air retention characteristics than above five fly ash samples. The gradual change in bed height confirms the ability to hold the air for longer time.

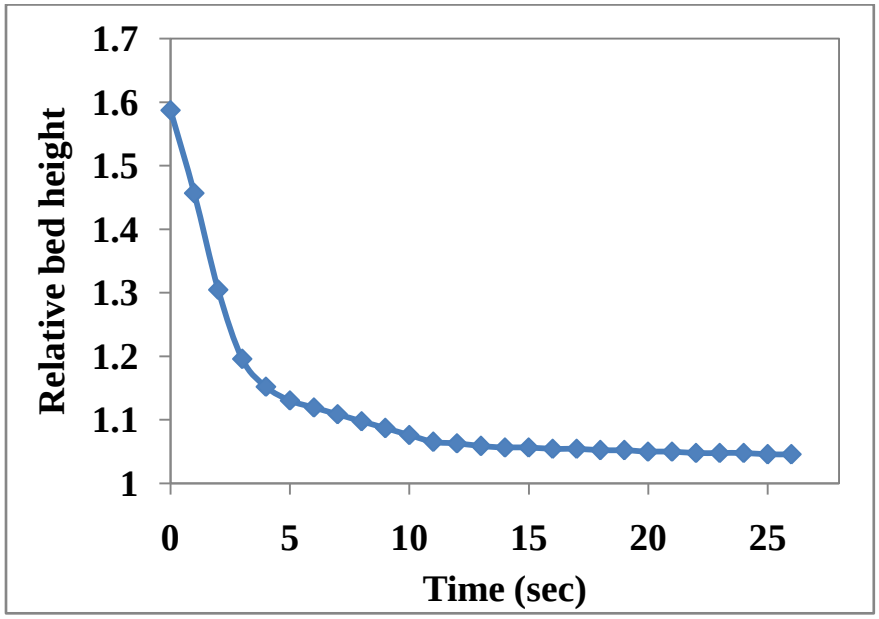

Figure 4.14: Drop in relative bed height vs. time for fly ash 7

The de-aeration characteristics of fly ash 7is shown in Figure 4.14 which clearly depicts that bed height decreased gradually due to small particle size and compaction of powders took place for a very long time indicating fly ash 7 having good air retention characteristics.

Based on the above finding, the powders having small median particle size would able to hold the air for much longer time than powders having larger median particle size which would de-aearte faster. It was found that fly ash 7 was most air retentive powder and fly ash 1 was least air retentive powders.

4.2.1 Pressure decay curves

The air retention characteristics of powders are measured more conveniently by investigating into pressure gradient when the air was instantaneously cut off.

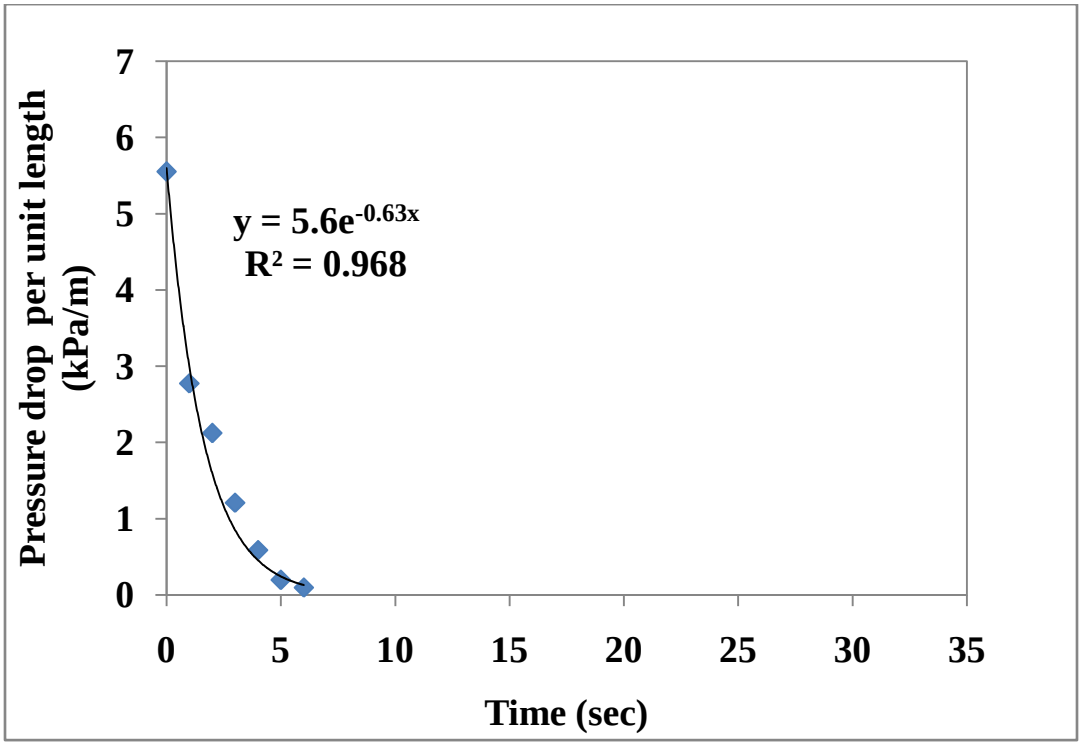

Figure 4.15: Pressure decay curve for fly ash 1

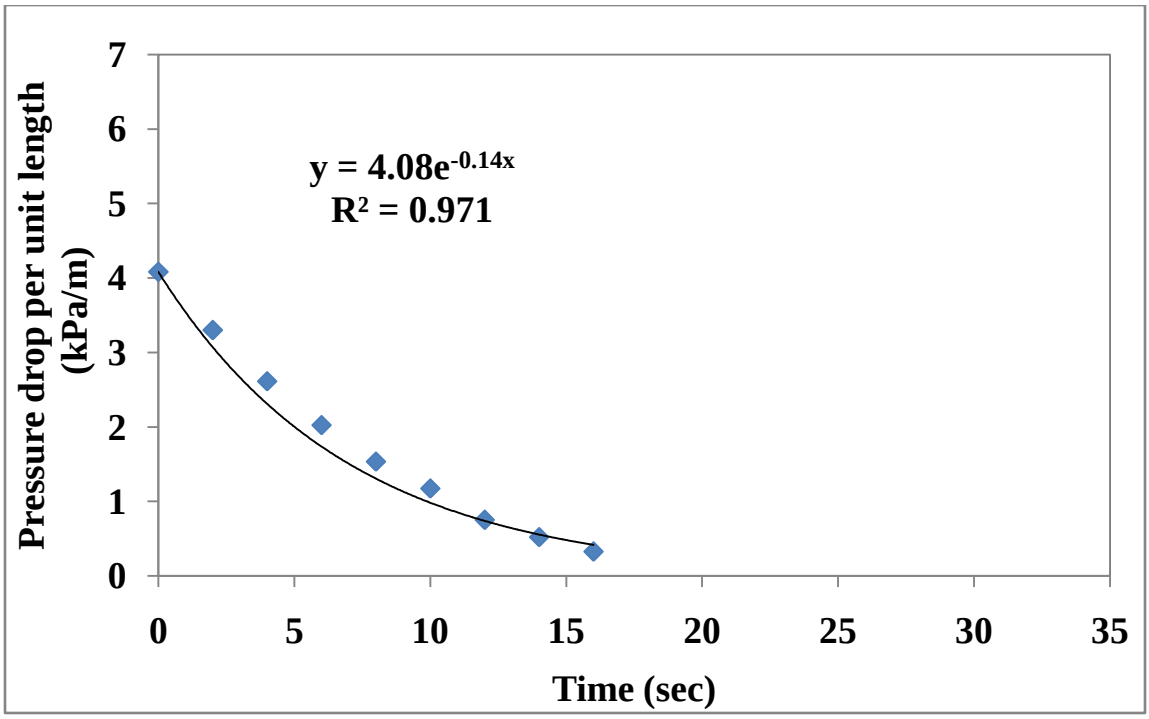

Figure 4.16: Pressure decay curve for fly ash 2

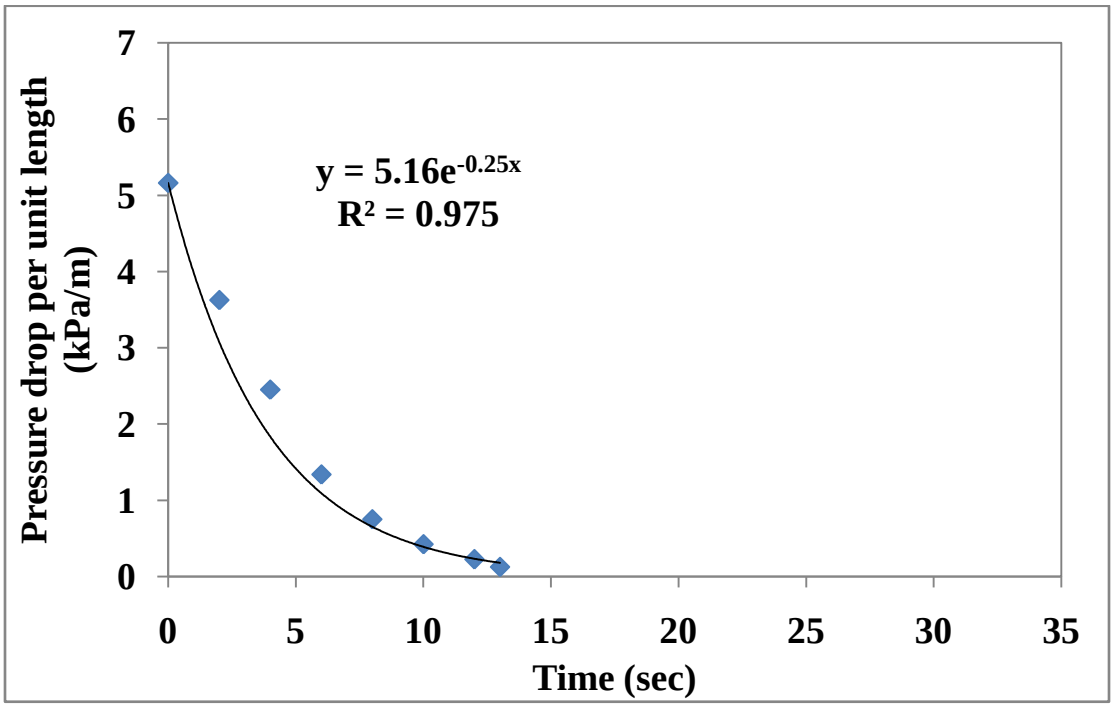

Figure 4.17: Pressure decay curve for fly ash 3

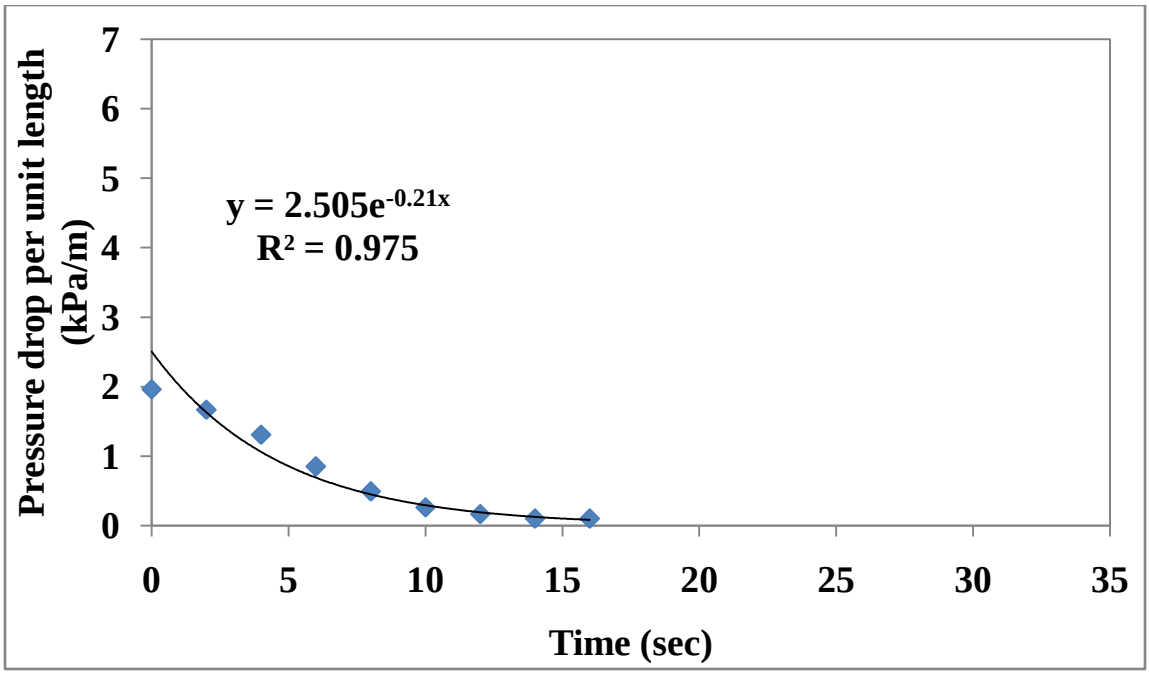

Figure 4.18: Pressure decay curve for fly ash 4

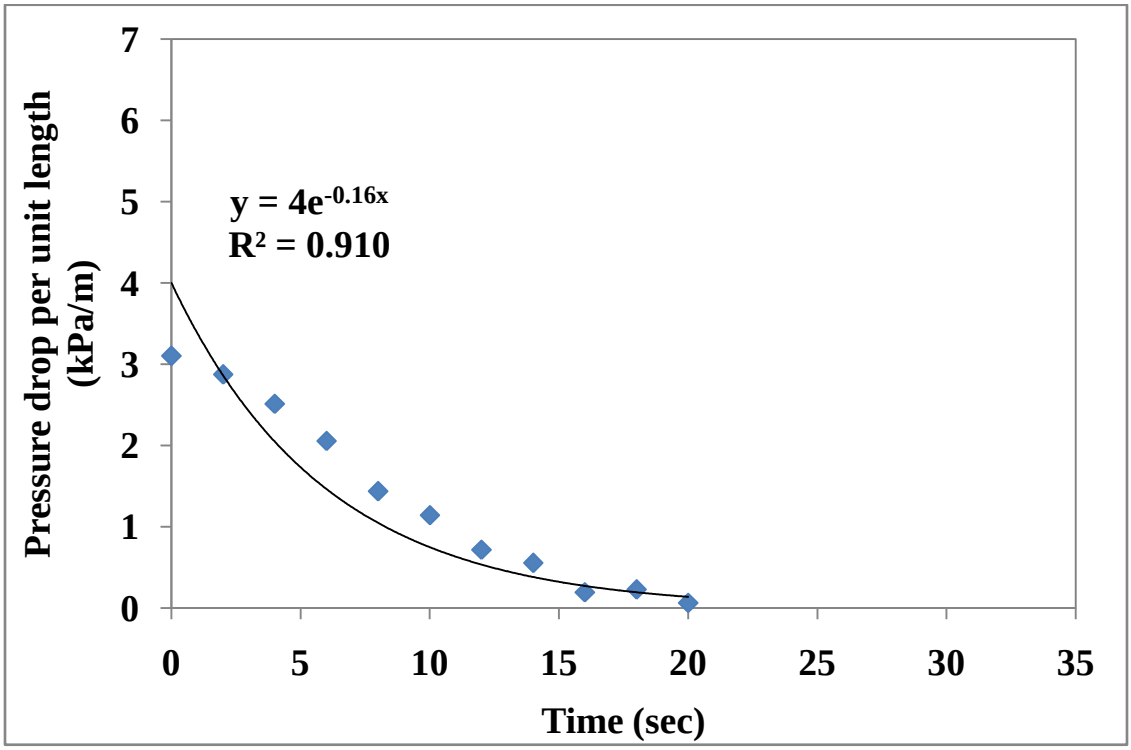

Figure 4.19: Pressure decay curve for fly ash 5

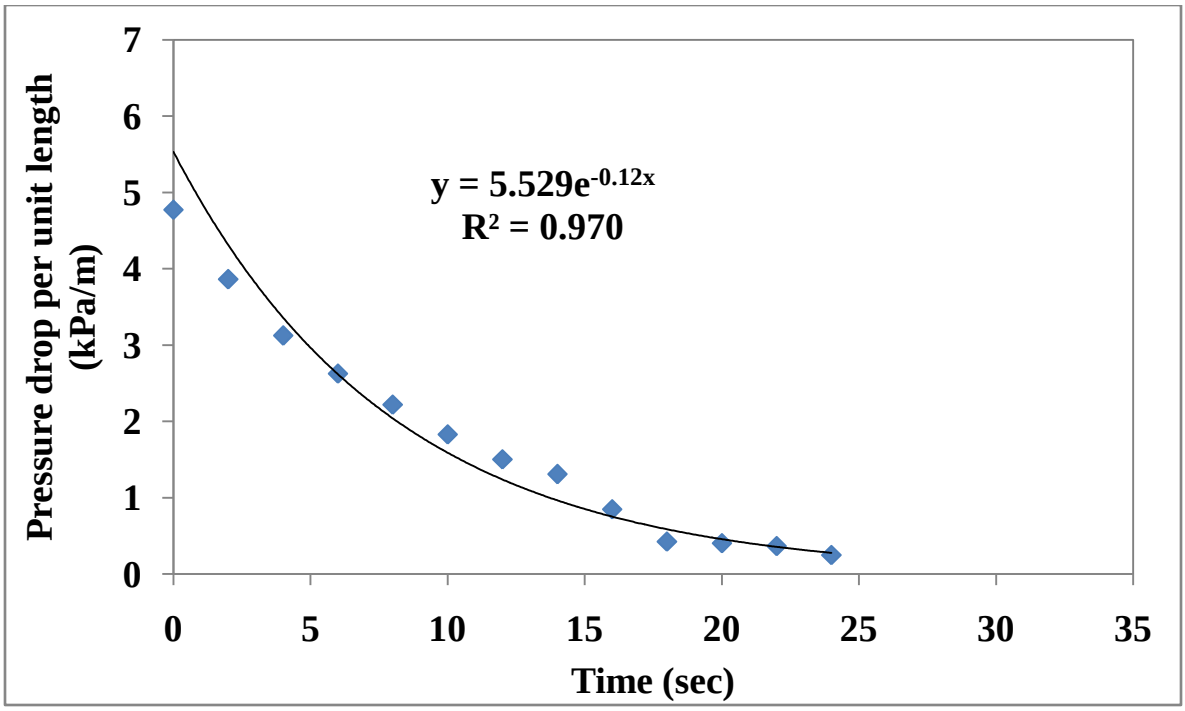

Figure 4.20: Pressure decay curve for fly ash 6

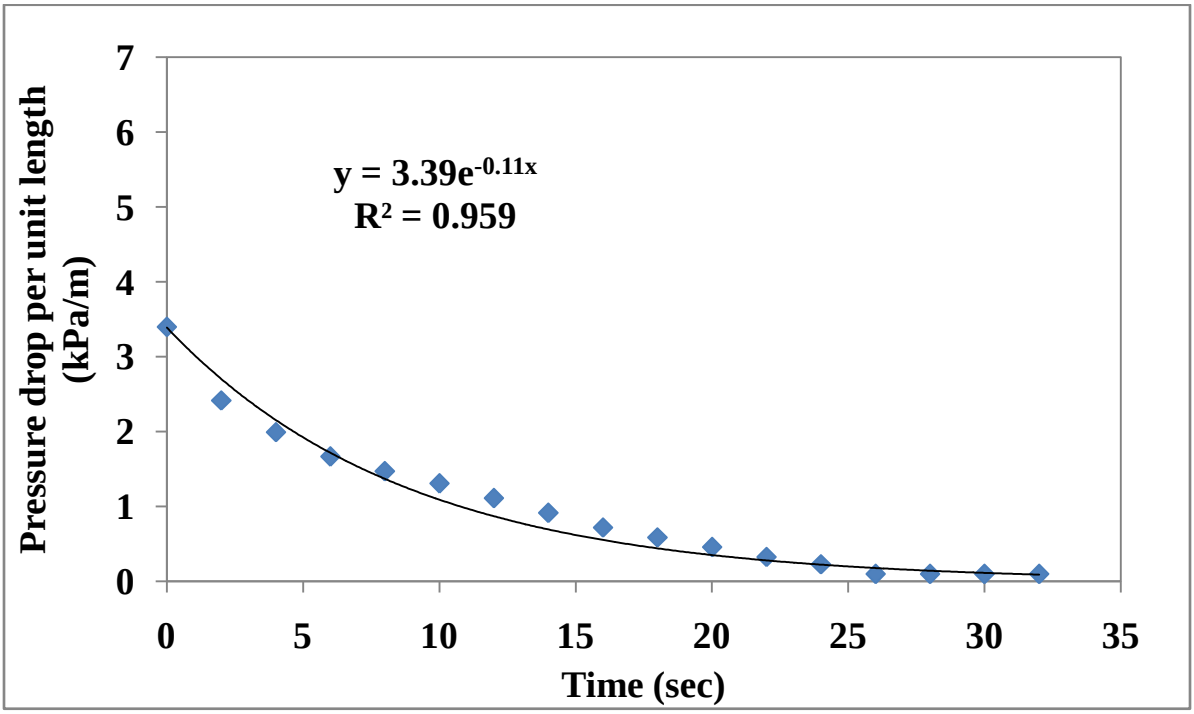

Figure 4.21: Pressure decay curve for fly ash 7

The de-aeration characteristics of different powders were studied by investigated into the pressure decay curve when the air was instantaneously cut off. Figure 4.15 to 4.21 represents the pressure decay curves for seven different samples of fly ash collected from different ESP hoppers of the same unit of thermal power station. The above analysis of seven different fly ash having different median size suggests that fly ash 7 collected from last hopper has the most air retention characteristics. The decay in pressure drop was more rapid in the case of large size particle as depicted in figure 4.15 and 4.16. This shows that fly ash 1 and fly ash 2 de-aerate faster. It was observed from Figure 4.9 that fly ash 2 relative bed height decreases very fast but figure 4.16 reveals that air was retained in fly ash 2 thus shows the larger time than relative bed height vs time curve. Figure 4.20 and 4.21 shows that these two powders were able to hold for much longer time than other powders thus having good de-aeration characteristics. It was found that all the powders follow an exponential decay in pressure drop against time with good value of R^2. The de-aeration time constant can be found from these exponential trend correlations shown in figure 4.15 to 4.21. It was found that fly ash 1 have lower de-aeration time constant of 1.58 and fly ash 7 have highest de-aeration time constant of 9.09. It also reveals that powders having larger values of de-aeration time constant retains air for significant amount of time. This characteristic of powders helps in easy conveying in pipelines rather than powders which would de-aerate fast.

CHAPTER 5: EVALUATION OF DIFFERENT MODELS FOR MINIMUM FLUIDIZATION VELOCITY

5.1 Introduction

The most generalized correlation for predicting the minimum fluidization velocity is given by Wen and Yu (1966) and presented by equation 2.5. This equation provides a general relationship between Reynolds number and Archimedes number. In the past, many researchers used this relationship to obtain different constants values relating Reynolds number and Archimedes number according to their own experimental data. Many theoretical and empirical models were developed by different researchers to obtain the value of minimum fluidization velocity. In this study four different correlations such as Abharamsen and Geldart (1980), Xie and Geldart(1995), Xu and Zhu (2008) and Vasconcelos and Mesquita(2011) along with Wen and Yu (1966) model were compared with the experimental values obtained for seven powders having different particle size of same material.

5.2 Evaluation of existing correlations for minimum fluidization velocity

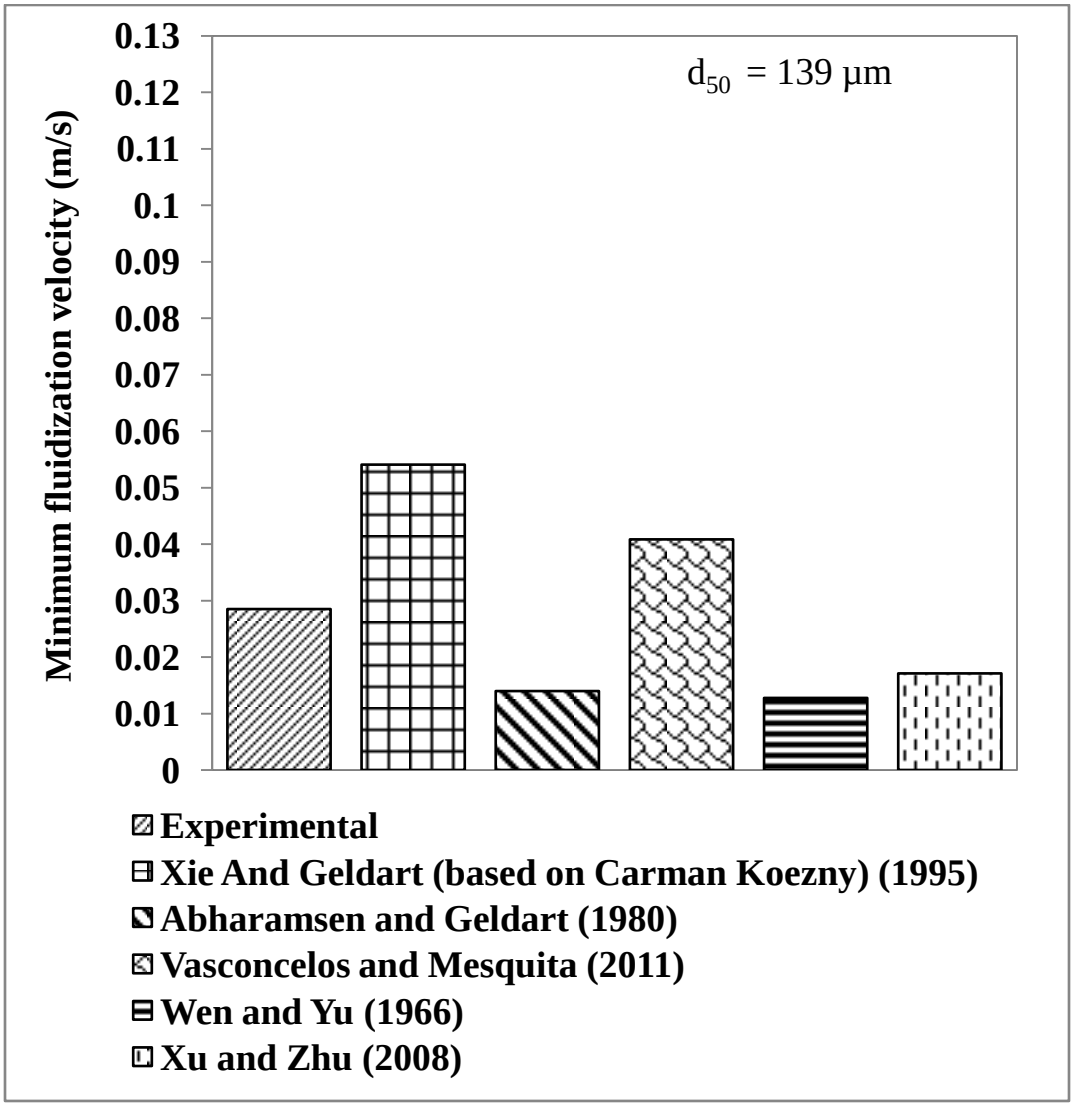

Figure 5.1: Comparison of experimental and predicted values of minimum fluidization velocity for fly ash 1 (ρ_s= 2015 kg/m^3,ρ_b= 848 kg/m^3,ε_{mf} = 0.5791)

Figure 5.1 showed that the correlations Xie and Geldart (1995) and Vasconcelos and Mesquita (2011) predicts the higher value of minimum fluidization velocity. Whereas, Wen and Yu (1966), Xu and Zhu (2008) and Abrahamsen and Geldart (1980) formulas under-predicts the value of U_{mf}. On the other hand, prediction made by Wen and Yu (1966) and Abrahamsen and Geldart (1980) show almost similar values for minimum fluidization velocity.

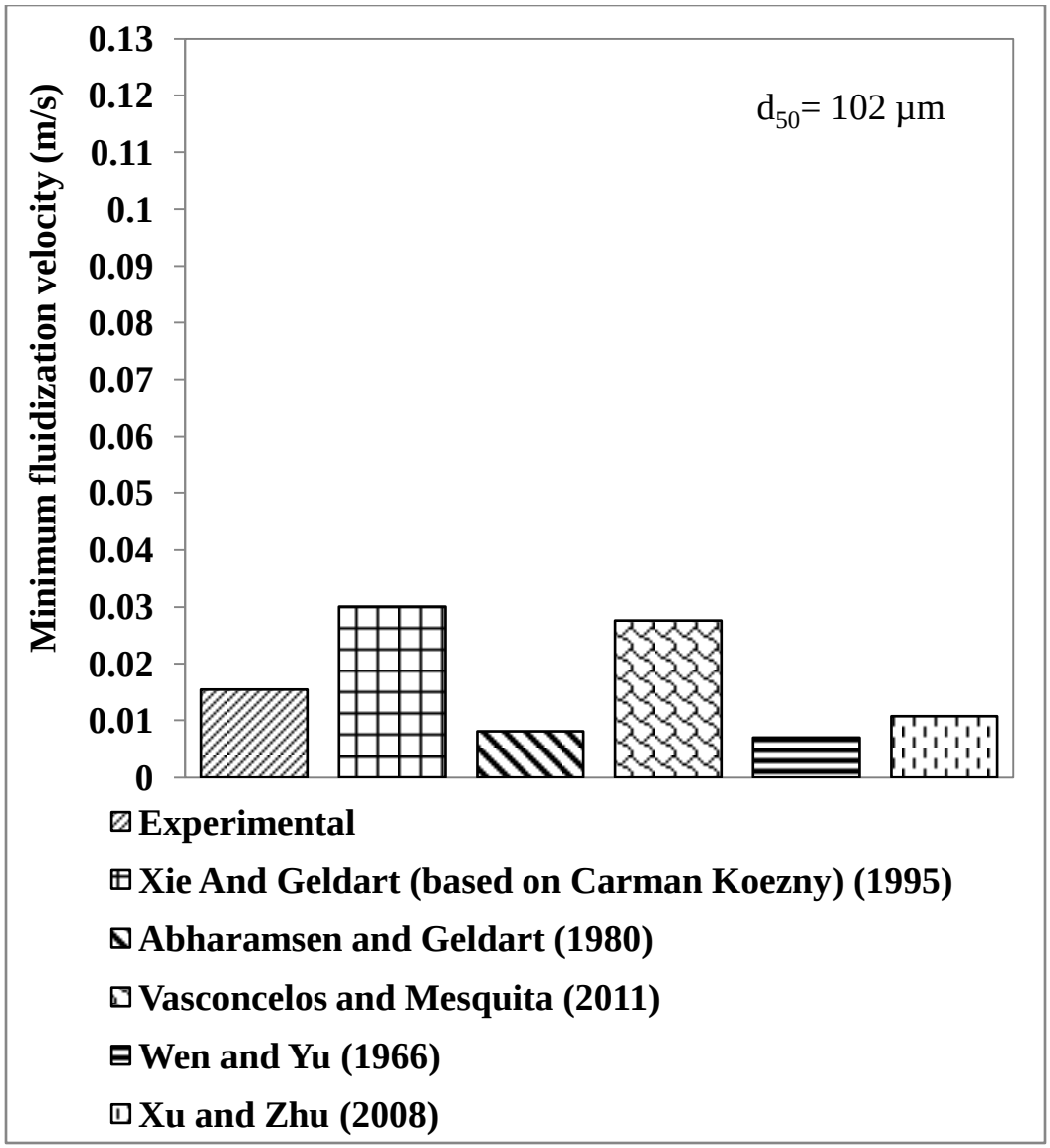

Figure 5.2 : Comparison of experimental and predicted values of minimum fluidization velocity for fly ash 2 (ρ_s= 2014 kg/m^3,ρ_b= 839 kg/m^3,ε_{mf} = 0.5834)

Figure 5.2 showed that experimental value when compared to some models to determine the minimum fluidization velocity. It was found that some correlations (Xie and Geldart,1995; Vasconcelos and Mesquita ,2011) gives over-predicted values and some models (Wen and Yu,1966 ; Abrahamsen and Geldart ,1980) gives under- predict the values of minimimum fluidization velocity. Whereas, Xu and Zhu (2008) correlation shows good prediction with experimental value of $U_{mf.}$.

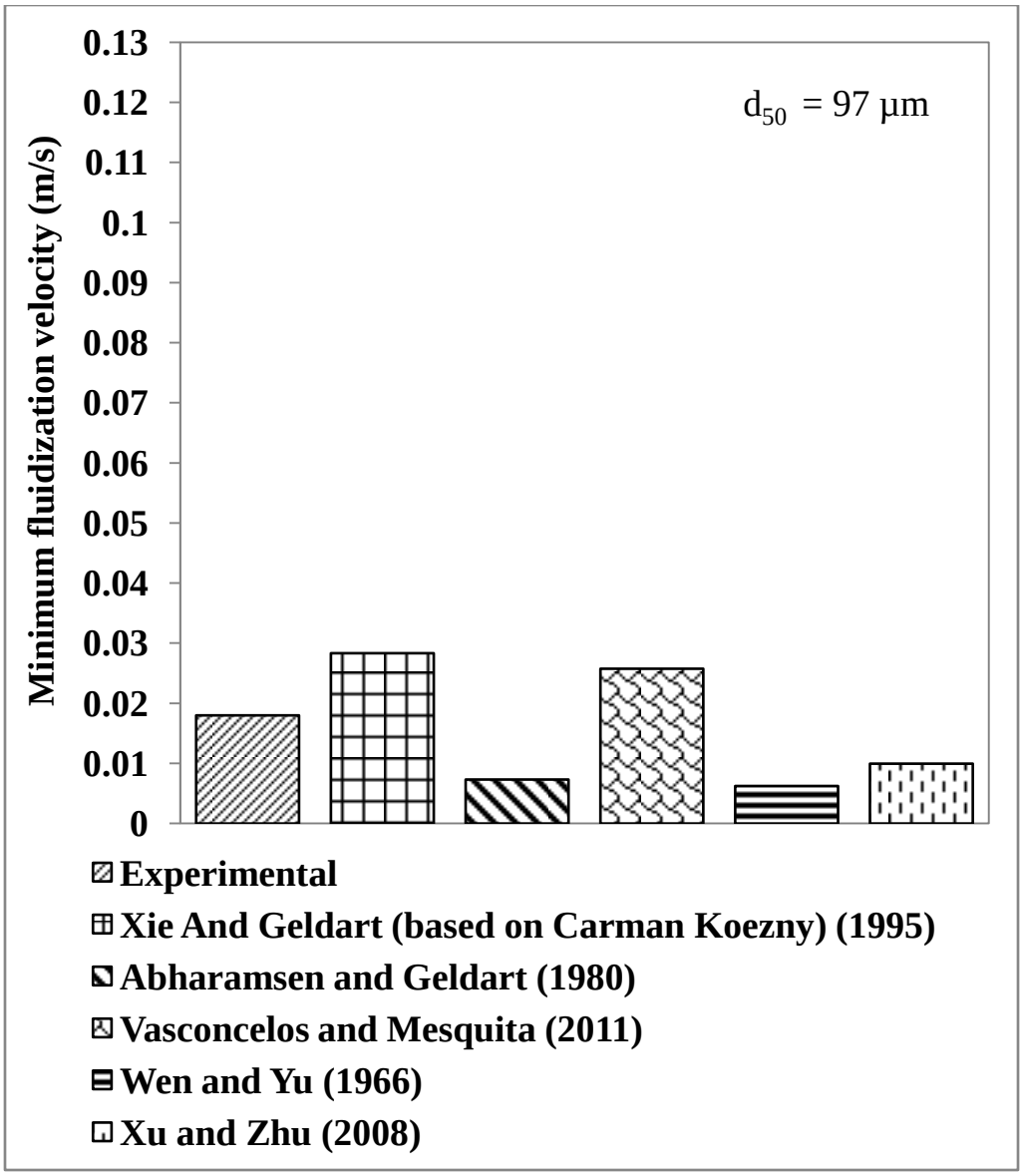

Figure 5.3: Comparison of experimental and predicted values of minimum fluidization velocity for fly ash 3 (ρ_s= 2018 kg/m^3,ρ_b= 830 kg/m^3,ε_{mf} = 0.5887)

In Figure 5.3 the experimental value for minimum fluidization velocity are compared with various empirical correlations available in literature for fine powders. It was found that Xie and Geldart (1995) correlations predict the highest value and Wen And Yu (1966) predicts the lower value for minimum fluidization velocity for fly- ash 3.

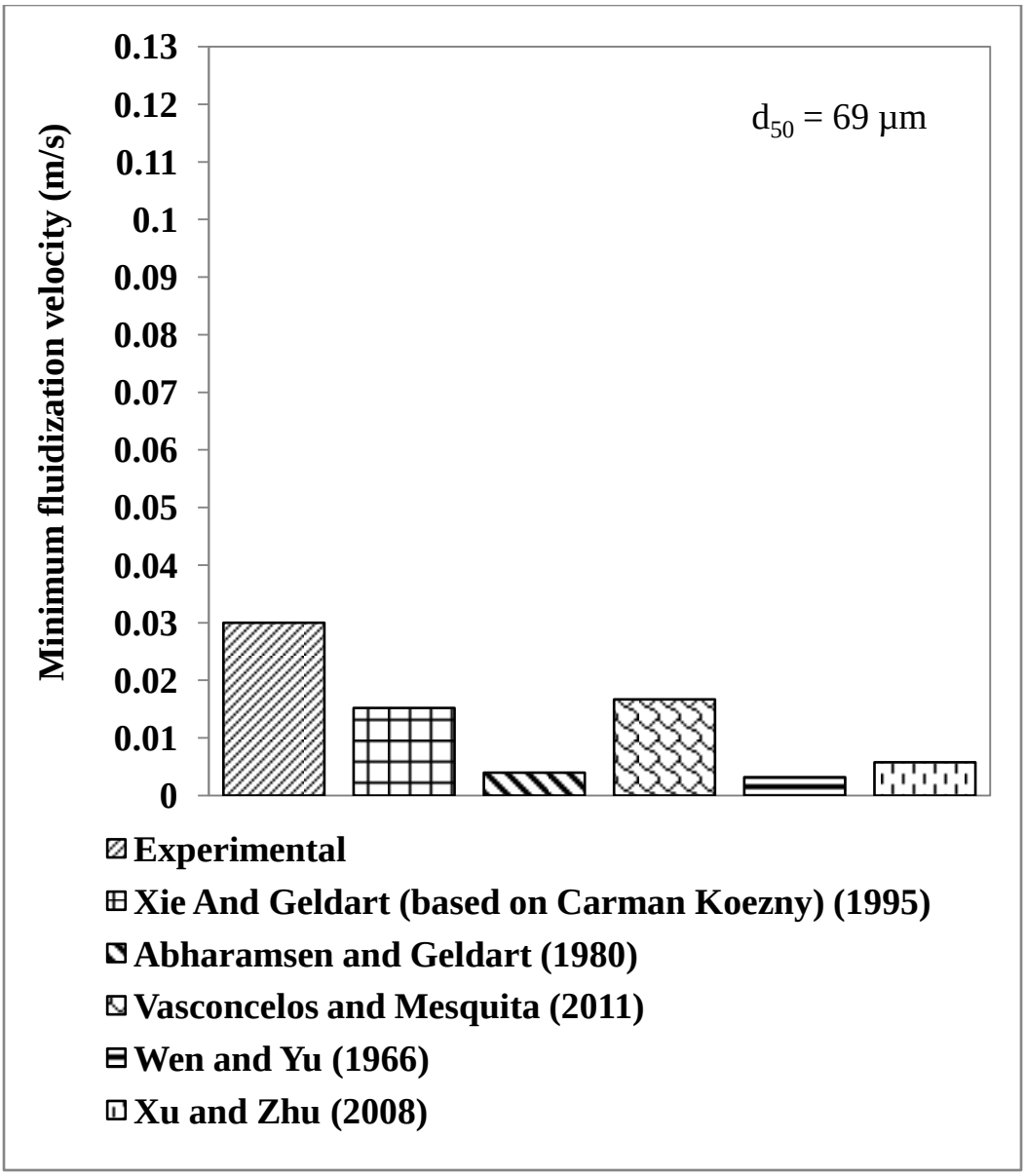

Figure 5.4: Comparison of experimental and predicted values of minimum fluidization velocity for fly ash 4 (ρ_s= 2025 kg/m^3,ρ_b= 818 kg/m^3,ε_{mf} = 0.5960)

Figure 5.4 shows the comparison of experimental and predicted values of minimum fluidization velocity. All the correlations used to find U_{mf} shows smaller values when compared to experimental value.

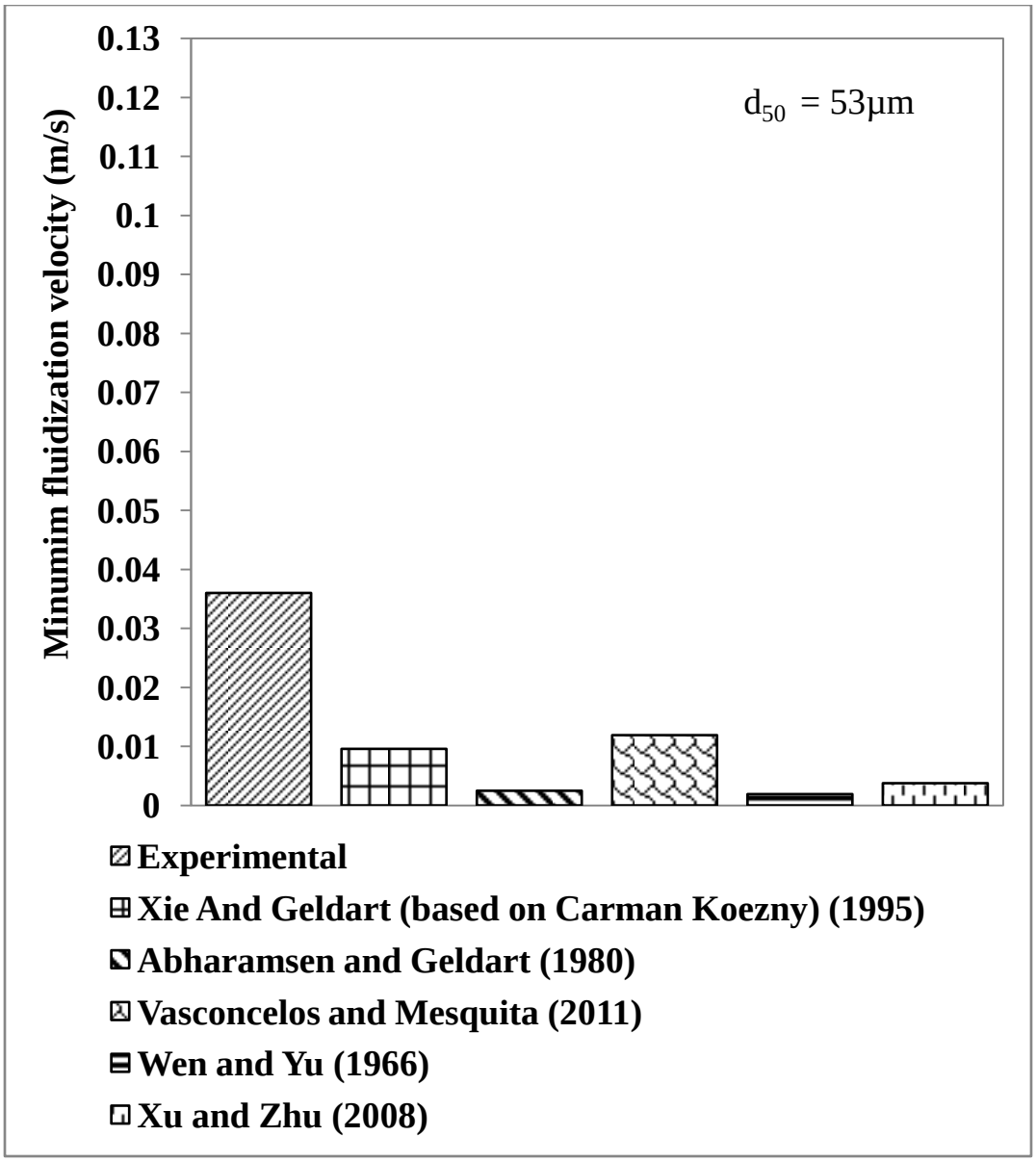

Figure 5.5: Comparison of experimental and predicted values of minimum fluidization velocity for fly ash 5 (ρ_s= 2032 kg/m^3,ρ_b= 805 kg/m^3,ε_{mf} = 0.6043)

Figure 5.5 shows that all the empirical models under-predicts the experimental value of minimum fluidization velocity. Whereas, Xie and Geldart (1995) and Vasconcelos and Mesquita (2011) models predicts approximately similar value for U_{mf}.

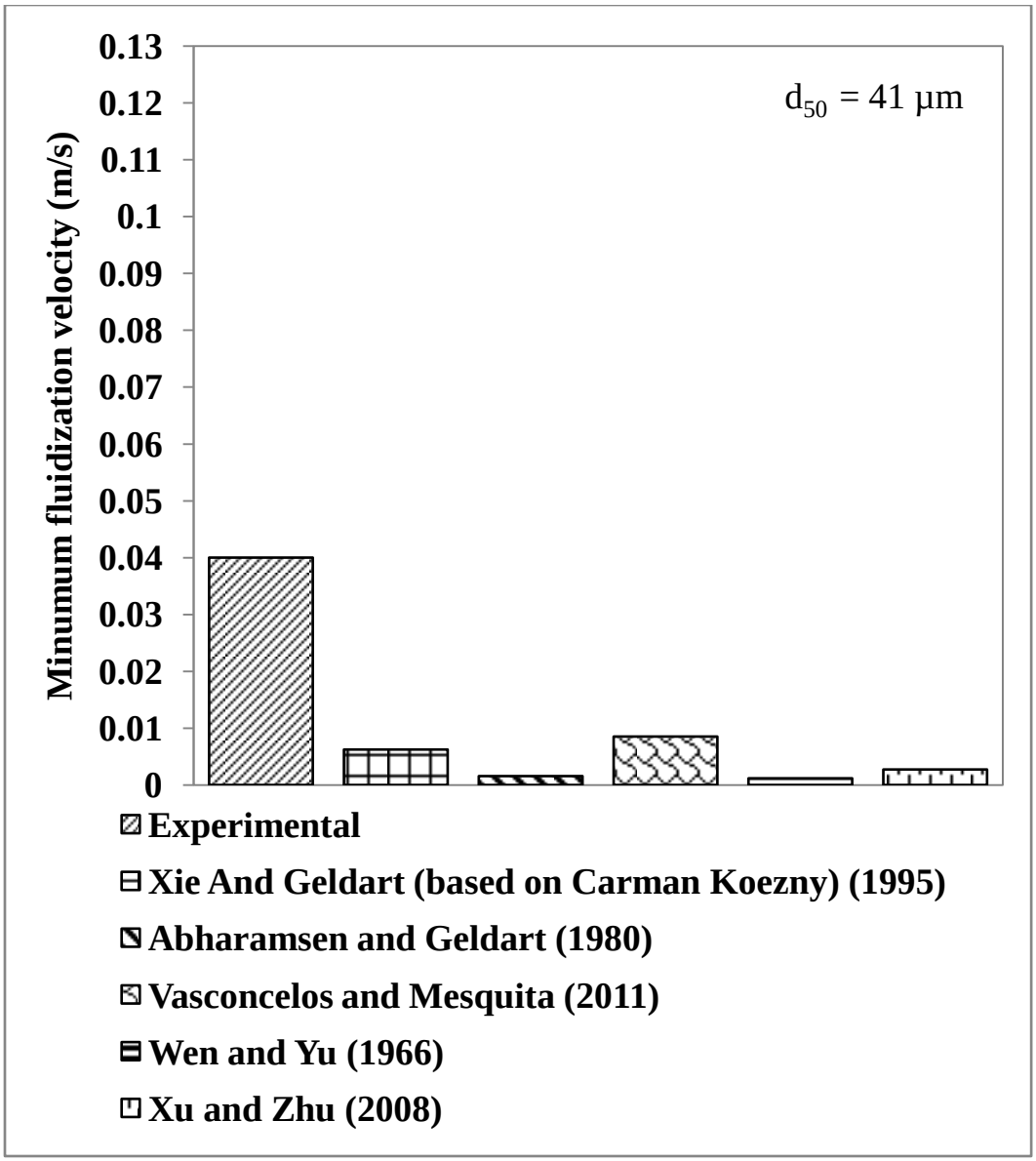

Figure 5.6: Comparison of experimental and predicted values of minimum fluidization velocity for fly ash 6 (ρ_s= 2030 kg/m^3,ρ_b= 780 kg/m^3,ε_{mf} = 0.6157)

Figure 5.6 shows that all the correlations under-estimated the experimental data , with Wen and Yu (1966) correlations provided the smallest value.

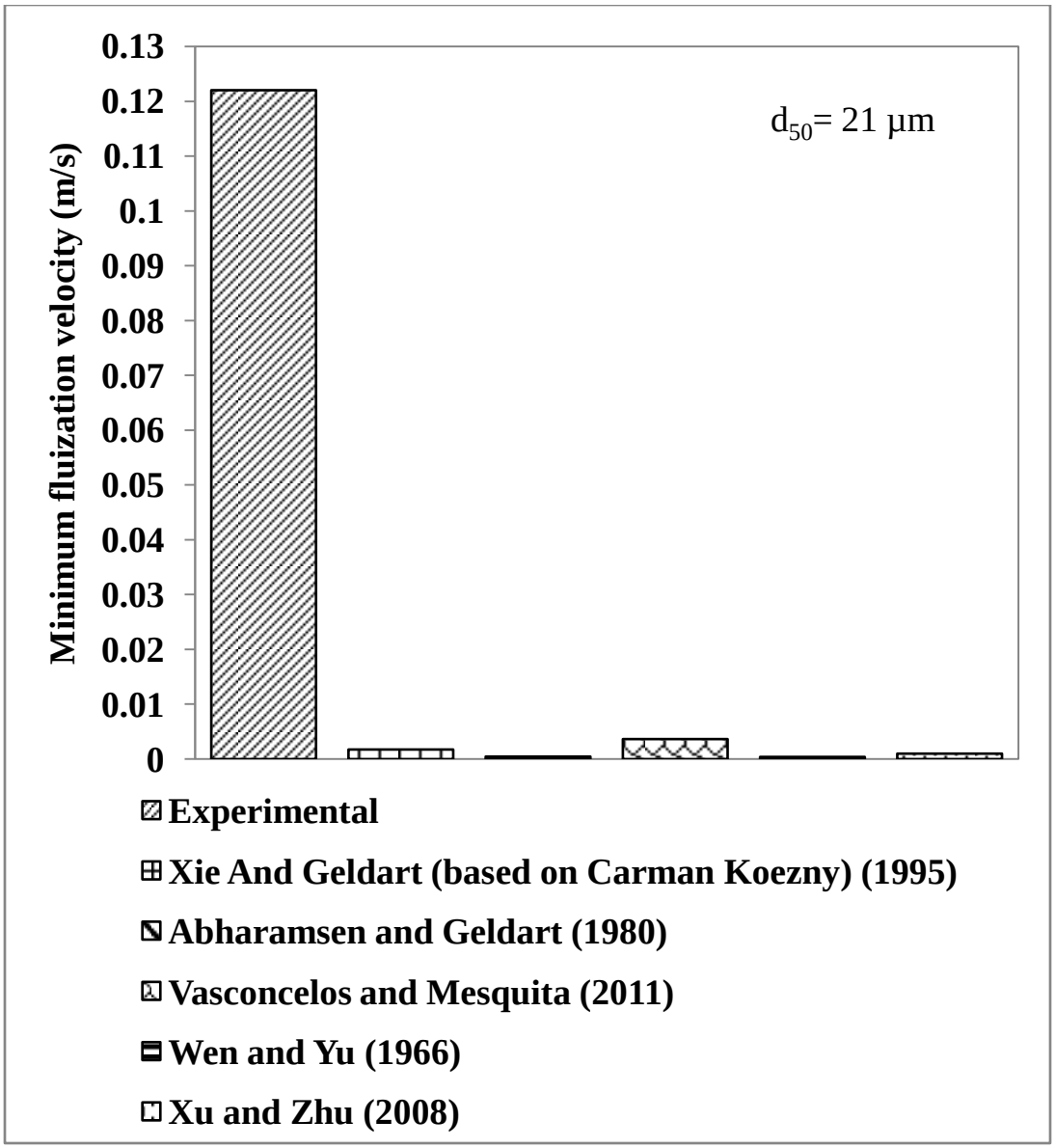

Figure 5.7: Comparison of experimental and predicted values of minimum fluidization velocity for fly ash 7 (ρ_s= 2025 kg/m^3,ρ_b= 759 kg/m^3,ε_{mf} = 0.6251)

Figure 5.7 shows the comparison plot of experimental and predicted value of minimum fluidization velocity for fly ash 7 having a smaller median particle size.It can be observed that all the models under predicts the value of minimum fluidization velocity.

5.2.1 Results and Discussion

The above comparison plots shows that different correlations can generate different predicted values of minimum fluidization velocities based on physical properties of that product. Figure 5.1 to 5.3 shows that Xie and Geldart (1995) and Vasconcelos and Mesquita (2011) models over predicted the value of minimum fluidization velocity for each product, whereas, Abhramsen and Geldart (1980), Wen and Yu (1966) and Xu and Zhu (2008) models underestimated the velocity of minimum fluidization for each product. All the models under predicted the minimum fluidization velocity value for fly ash 4,5,6,7 (figure 5.4 to 5.7). The reasons for under estimation could be the strong inter- particle forces acting between the particles which were not considered in the models. All the models provided relatively larger disagreements for fly ash 7. The reasons for this large deviation could be that fly ash 7 belongs to Geldart category C, which is cohesive, having strong inter-particle forces. The particles might have stayed in agglomerated form during experiments; thus the size of agglomerates was larger than primary particle size, which would tend to result in higher experimental values of minimum fluidization velocity Also the minimum fluidization velocity was influenced by several factors such as density, gas- solid interactions, particle shape, particle- particle interaction, friction between wall and particle etc. It was observed from above comparison plots that none of the correlations predicted the similar value for minimum fluidization velocity as obtained from experiments because each correlation was derived in different experimental condition and for different particles.

CHAPTER 6: CONCLUSION AND FUTURE SCOPE OF WORK

6.1 Conclusion

Fluidization and De-aeration characteristics of different median particle size of fly ash were studied. It can be concluded that -

- The minimum fluidization velocity was strongly dependent on particle size distribution. As particle size decreased from 139 to 102 μm, there was a considerable reduction in experimentally determined values of minimum fluidization velocity. Further decrease in particle size led to an increase in minimum fluidization velocity due to the effect of stronger inter-particle cohesive forces that are typically present in fine powders. The fly ash with the least median size (21μm) showed channeling and agglomeration during fluidization.
- The value of permeability factor was obtained from slope of fluidization curve.It has been found that fly ash 7 gives higher value of permeability factor thus showing plug formation during initial stage of fluidization whereas fly ash 3 gives lowest value of permeability factor.
- De-aeration test results showed that fly ash 1 has less ability to retain air due to larger particle size, whereas fly ash 7 shows that there was a gradual decrease in relative bed height and pressure drop per unit length against time because the particle size is small hence slow de-aeration took place. The characteristic time constant values obtained from pressure decay curves also reveals that powders having larger values were able to hold air for much longer time than the powders having smaller value for time constant that would de-aerate faster.
- Existing models for predicting minimum fluidization velocity under-estimated the same for the 21μm sized fly ash (fine powder in Geldart Group C category) due to the cohesive

bonding of fine powders that requires higher gas flows (compared to model predictions) to initiate fluidization.

- The fly ash sample with 139 µm particle size seems to be a dilute-phase product; i.e. can not be possibly conveyed in fluidized dense-phase (due to poor fluidization and air retention properties). The fly ash samples with 69,53,41,21 µm seem to be good dense-phase materials; however, the 21 µm ash can be cohesive could have flowability problems. The 102 µm and 97 µm ash are a border-line materials between dense and dilute-phase and should exhibit some dense-phase conveyability, but would require higher conveying velocity to maintain the flow (i.e. to prevent line blockage).

6.2 Future scope of work

i. Further research needs to be carried out on different fly ash samples to better understand the mechanism of fluidization and de-aeration.

ii. A model for minimum fluidization velocity of fly ash has to be developed by taking into consideration various factors such as inter-particle forces, density, particle size, viscosity, cohesiveness etc.

REFERENCES

Abrahamsen, A.R. and Geldart, D. (1980). Behavior of Gas Fluidized Beds of Fine Powders Part I.Homogenous expansion. Powder Technology. 26: 35-46.

Baretta, D., Donsi, G., Ferrari, G. and Polleto, M. (2007). A Rotational Tester For Characterization of Aerated Shear Flow of Powders. 24: 259-270.

Chen, W. (2013). PHD Dissertation. The Rheology of Aerated Fine Powders: Theory And Application In Pneumatic Conveying Systems. University of Newcastle.

Geldart , D. (1973) . Types of Gas Fluidization. Powder Technology. 7: 285-292.

Geldart, D., Harnby, N. and Wong, A.C. (1984). Fluidization of Cohesive Powders. Powder Technology. 37: 25-37.

Gupta, S.K., Agarwal, V.K., Singh, S.N., Mills, D., Singh, J. and Prakash, C. (2009). Prediction of Minimum Fluidization Velocity for Fine Tailing Materials. Powder Technology. 196: 263-271.

Hirota, M., Sogo, Y., Marutani, T. and Suzuki, M. (2002). Effect of Mechanical Properties of Powders on pneumatic Conveying in Inclined Pipe. Powder Technology. 122: 150-155.

Jones, M.G. and Mills, D. (1990). Product Classification for Pneumatic Conveying. Powder Process and Handling. 2(2): 117-122.

Jones, M.G. and Williams, K.C. (2008). Predicting the Mode of Flow in Pneumatic Conveying System- A Review. Particuology. 6: 289-300.

Kennedy, O.C, The Deaeration Behaviour of Bulk Solids – the Time Constant as a Characterizing Parameter, The Proceeding of Sixth International Conference on Bulk Materials storage, Handling And Transportation Wollongong NSW, Australia, 28-30 September (1998): 303-308.

Kennedy, O.C and Wypych, P.W. Course Notes on Characterization and Classification of Bulk Solids. University of Wollongong.

Klinzing, G.E., Rizk, F., Marcus, R. and Leung, L.S. (2009). Pneumatic Conveying of Solids. Publ. Springer. 3rd Ed.

Kenneth, W.C. (2008). PHD Dissertation: Dense Phase Pneumatic Conveying of Powders: Design Aspect and Phenomena, University of Newcastle.

Leturia, M., Benali, M., Lagarde, S., Ronga. I., Saleh, K., (2014). Characterization of Flow Properties of Cohesive Powders: A Compartive study of Traditional and New Testing Methods. Powder Technology. 253: 406-423

Liu,H., Zhang, L., Chen, T., Wang,S., Han, Z. and Wu, S. (2015). Experimental Study on the Fluidization Behavior of the Superfine Particles. Chemical Engineering Journal. 262: 579-587.

Mainwaring, N.J. and Reed, A.R. (1987). Permeability and Air Retention Characteristics of Bulk Solids Materials in Relation to Modes of Dense Phase Pneumatic Conveying. Bulk Solids Handling. 7 (3): 415-425.

Mallick, S.S. (2009). PhD Dissertation: Modelling dense-phase pneumatic conveying of powders. University of Wollongong, Australia.

Pan, R. (1999). Material Properties and Flow Modes in Pneumatic Conveying. Powder Technology. 104: 157-163.

Rabinovich, E. and Kalman, H. (2011). Flow Regimes Diagram for Vertical Pneumatic Conveying and Fluidized Bed Systems. Powder Technology. 207: 119-133.

Sanchez, L., Vasquez, N., Klinzing, G.E. and Dhodapkar, S. (2003). Characterization of Bulk Solids to Asses Dense Phase Pneumatic Conveying. Powder Technology. 138: 93-117.

Schulze, D. (2007). Powders and Bulk Solids. Publ. Springer.

Vasconcelos, P.D. and Mesquita, L. (2011). Minimum and Full Fluidization Velocity for Alumina Used in the Aluminum Smelter. International Journal of Engineering Business Management. 3: 7-13.

Wen, C.Y. and Yu, Y.H. (1966). A Generalized Method of Predicting Minimum Fluidization Velocity. AICHE Journal. 12(3): 610-611.

Wypych, P.W. (1989). PhD. Dissertation: Pneumatic Conveying of Bulk Solids. University of Wollongong, Australia

Wypych, P.W. (2006). Course Notes on Introduction to Pneumatic Conveying. University of Wollongong.

Xie, H.Y. and Geldart, D. (1995). Fluidization of FCC Powders in Bubble-Free Regime: Effect of Type of Gases and Temperature. Powder Technology. 82: 269-277.

Xu, C. and Zhu, J. (2006). Parametric Study of Fine Particle Fluidization under Mechanical Vibration. Powder Technology. 161: 135-144.

Xu, C. and Zhu, J. (2008). Prediction of the Minimum Fluidization Velocity for Fine Particles of Various Degrees of Cohesiveness, Chemical Engineering Communications Taylor & Francis. 196(4): 499-517.

COMMUNICATIONS

Chawla, A., Setia, G. and Mallick, S.S. An Experimental Investigation into the Effects of Particle Size on the Fluidization and De-aeration Characteristics of Powders to Assess Dense-Phase Pneumatic Conveyability. **Powder Technology, Elsevier.**